REPORT DOCUMENTATION PAGE

Form Approved
OMB NO. 0704-0188

Public Reporting burden for this collection of information is estimated to average 1 hour per response, including the time for reviewing instructions, searching exist ing data sources, gathering and maintaining the data needed, and completing and reviewing the collection of information. Send comment regarding this burden estimates or any other aspect of this collection of information, including suggestions for reducing this burden, to Washington Headquarters Services, Directorate for information Operations and Reports, 1215 Jefferson Davis Highway, Suite 1204, Arlington, VA 22202-4302, and to the Office of Management and Budget, Paperwork Reduction Project (0704-0188,) Washington, DC 20503.

1. AGENCY USE ONLY (Leave Blank)	2. REPORT DATE	3. REPORT TYPE AND DATES COVERED
	August 8, 2001	Final Progress Report, Sept.1, 1996 – May 31, 2001

4. TITLE AND SUBTITLE
Spectroscopic studies of novel materials for display and NLO applications

5. FUNDING NUMBERS
DAAH04-96-1-0416

6. AUTHOR(S)
Huimin Liu

7. PERFORMING ORGANIZATION NAME(S) AND ADDRESS(ES)
Department of Physics, University of Puerto Rico, Mayaguez, PR 00681

8. PERFORMING ORGANIZATION REPORT NUMBER

9. SPONSORING / MONITORING AGENCY NAME(S) AND ADDRESS(ES)

U. S. Army Research Office
P.O. Box 12211
Research Triangle Park, NC 27709-2211

RECEIVED
AUG 0 8 2001
By

10. SPONSORING / MONITORING AGENCY REPORT NUMBER
36379.37-MS-DPS

11. SUPPLEMENTARY NOTES
The views, opinions and/or findings contained in this report are those of the author(s) and should not be construed as an official Department of the Army position, policy or decision, unless so designated by other documentation.

12 a. DISTRIBUTION / AVAILABILITY STATEMENT
Approved for public release; distribution unlimited.

12 b. DISTRIBUTION CODE

13. ABSTRACT (Maximum 200 words)

During the grant period our research was organized into three thrust areas: Material preparation; nonlinear optical characterization; and luminescence studies on display materials. We successfully prepared, KN, KTN, SBN etc. photorefractive materials in the form of thin films using pulsed laser deposition (PLD) technique through collaboration with professor sharing our laboratory. We also used sol-gel technique and laser-pedal crystal growth to prepare some luminescent material and Low voltage cathodoluminescent phosphors. During the period we systematically studied the ultrafast nonlinear optical response with purpose in searching for larger third-order nonlinearity, and found significant enhancement of SBN in the form of thin film. Based on the experimental observation a charge-transferred-vibronic model was successfully developed. We also discovered valence switching by charge carriers produced in CB and captured by ions residing on the boundary surface in nanostructured materials. The study of luminescent materials for display applications was extended to $SrAl_2O_4$: $CaAl_4O_7$:Eu^{3+}. Eu^{2+},Dy^{3+}, and long-lifetime display materials were developed. It was found that the excitation by high UV flux can produce higher density of electrons near the grain boundary, which may further enhance the indirect transition probability or increase energy transfer from surface states to the SA centers of the host.

14. SUBJECT TERMS	15. NUMBER OF PAGES
Spectroscopy, Nonlinear optical properties, Display, Charge transfer	65
	16. PRICE CODE

17. SECURITY CLASSIFICATION OR REPORT	18. SECURITY CLASSIFICATION ON THIS PAGE	19. SECURITY CLASSIFICATION OF ABSTRACT	20. LIMITATION OF ABSTRACT
UNCLASSIFIED	UNCLASSIFIED	UNCLASSIFIED	UL

NSN 7540-01-280-5500

Standard Form 298 (Rev.2-89)
Prescribed by ANSI Std. 239-18
298-102

20010831 026

SPECTROSCOPIC STUDIES OF NOVEL MATERIALS FOR DISPLAY AND NLO APPLICATIONS

FINAL PROGRESS REPORT FOR PERIOD

September 1, 1996 - May 31, 2001

(DAAH04-96-1-0416)

Huimin Liu, Ph.D
PI, Professor of Physics
Department of Physics
University of Puerto Rico
Mayaguez, PR 00681

August 2001

MASTER COPY: PLEASE KEEP THIS "MEMORANDUM OF TRANSMITTAL" BLANK FOR REPRODUCTION PURPOSES. WHEN REPORTS ARE GENERATED UNDER THE ARO SPONSORSHIP, FORWARD A COMPLETED COPY OF THIS FORM WITH EACH REPORT SHIPMENT TO THE ARO. THIS WILL ASSURE PROPER IDENTIFICATION. NOT TO BE USED FOR INTERIM PROGRESS REPORTS; SEE PAGE 2 FOR INTERIM PROGRESS REPORT INSTRUCTIONS.

MEMORANDUM OF TRANSMITTAL

U.S. Army Research Office
ATTN: AMSRL-RO-BI (TR)
P.O. Box 12211
Research Triangle Park, NC 27709-2211

☐ Reprint (Orig + 2 copies)

☐ Technical Report (Orig + 2 copies)

☐ Manuscript (1 copy)

X Final Progress Report (Orig + 2 copies)

☐ Related Materials, Abstracts, Theses (1 copy)

CONTRACT/GRANT NUMBER: DAAH04-96-1-0416

REPORT TITLE: Spectroscopic studies of novel materials for dsplay and NLO applications.

SUBMITTED FOR PUBLICATION TO (applicable only if report is manuscript):
ARO

Sincerely,

TABLE OF CONTENTS

2. STATEMENT OF THE PROBLEMS STUDIED

During the grant period the problems studied are classified as follows:

1) Material preparation.

a. Using sol-gel technique to approach the high-efficient display materials

b. Using pulsed-laser-deposition technique to prepare the material in the form of thin films which showing enhanced third-order nonlinearity.

c. Using sputtering and melting technique to obtain nanostructure material and inorganic glass which is suitable for optical memory applications.

2) Nonlinear optical spectroscopic studies

a. Studied ABO_3 perovskite and SBN, KNSBN ferroelectric crystals, to understand the mechanism causing the anomalous NLO behaviors.

b. Studied SBN in the form of thin film and obtained enhanced NLO.

c. Characterized nonlinear hot-luminescence from Mn in ZnS

d. Studied Eu-doped c-Si/SiO_2 nanoparticle thin films and showing interesting valence switching.

3) Luminescence materials

a. Studied transition metal ions and rare-earth ions doped glass-ceramics and to understand the luminescence efficiency affected by host composition and additional dopants.

b. Characterized photoemission of 4f ions in Al_2O_4 host and in other ZnO materials for display applications.

4) Theoretical model developed: Charge Transferred Vibronic Exciton model has been developed and well applied in interpretation of NLO behavior in ferroelectric materials.

3. SUMMARY OF THE MOST IMPORTANT RESULTS

I. MATERIAL PREPARATION:

Three types of materials we prepared during this calendar year. They are 1)Multilayed thin films of mixed crystal of SBN and KTN types of niobate, titanate and tantalate for nonlinear optical studies. 2) Display materials. 3) Sol-gel based glass doped with rare-earth and transition metal ions in the form of nanostructural materials for laser application.

1) Thin films of mixed crystal of SBN and ABO_3 types of niobate.

The mixed-crystal family $Sr_xBa_{1-x}Nb_2O_6$ (SBN) is one of the most important photorefractive materials. It exhibits an exceptionally large diagonal electro-optic (E-O) coefficient r_{33} compared to all E-O crystals reported to date, and therefore has a strong potential for applications in optical data storage, switching and optical computing. For amorphous SBN thin films with x=0.61 we have recently obtained evidence of a considerable enhancement of $\chi^{(3)}$, by 2 orders of magnitude, with respect to bulk crystal values [1,2]. One advantage of having good NLO properties in amorphous or fine-grained polycrystalline films is that this simplifies multilayer growth considerations, making it possible to use ordinary glasses as linear materials in the stack. SBN and other multicomponent oxides which have attractive third-order NLO properties can be successfully grown by Pulsed Laser Deposition. Our PLD system, described below, allows for computer-controlled deposition of multilayers with up to 4 different materials. On the other hand, another interesting possibility in this material relates to its use as a host for Eu^{3+} ions in relation to the large quadrupole splitting and spin-lattice relaxation times which make Eu^{3+} attractive in hole burning experiments [3]. The practical importance of such system lies in the proposed application for a frequency domain information storage as well as for persistent OL applications. Very recently, we conducted spectral hole-burning experiments on Eu^{3+} -doped amorphous SBN thin films prepared by PLD. An inhomogeneous line width of FWHM = 13 Å was obtained in the excitation spectrum. The

spectral hole burned in the film had a width of ~100 MHz and depth of 30%. These results have stimulated the interest in extending this work for Eu-doped thin films prepared at a range of conditions in order to obtain the spectral hole burning effect at higher temperatures.

Potassium tantalate and potassium niobate are of particular interest among perovskite-structure ABO_3 materials because their para- or ferroelectric properties can be drastically altered by small changes in structure introduced either mechanically, by stress, or chemically, by introducing other ions. Development of PLD in the last decade has permitted the successful preparation of niobate and tantalate thin films deposited onto a variety of substrates. This offers great opportunities to study the variation of optical properties with structural changes. PLD-grown KTN ($KTa_{1-x}Nb_xO_3$) thin films have shown dramatic changes in second-order as well as the third-order nonlinearity. We have systematically studied the nonlinear optical (NLO) properties of pure $KTaO_3$, $KNbO_3$, as well as mixed crystal KTN [4,5]. More recently, we investigated the nonlinear optical response of a $KNbO_3/KTaO_3$ superlattice grown by PLD on a (001)-oriented $KTaO_3$ substrate. The difference in NLO response between bulk $KTaO_3$ and the superlattice was measured, and the $\chi^{(3)}$ value was estimated to have increased by 2 orders of magnitude compared to the bulk crystal [6]. In extending our work with KTN and $KNbO_3/KTaO_3$ superlattices we will be interested in probing dynamical processes in these structures by doping with rare earth or 3d ions. With energy donor and acceptor ions as dopants in alternate layers, nonequilibrium phonons with given modes produced during excitation will be confined within the layer boundaries, resulting in a substantial reduction of phonon free path. Phonon-phonon scattering within a single layer will therefore be enhanced. Penetration of layers by phonons associated with certain modes are of interest in order to study the mechanism of phonon-assisted energy transfer in a reduced dimensionality environment. Many efforts have been undertaken to produce KTN family materials. In our Lab, the use of pulsed laser deposition (PLD) for thin film growth in research applications is currently available through the collaboration with Dr. Felix Fernandez. This technique has been shown to produce very high quality films. The system core is a small (25 liter) 304 stainless steel ultra-high vacuum chamber. The

chamber is pumped by a differential-ion pump, with integral baking heaters, and rough-pumped by dual sorption pumps. This extremely clean system, designed to allow future surface analysis studies, is capable of reaching vacua in the low 10^{-10} Torr region. A quadrupole mass analyzer monitors residual gasses in the chamber. The UHV chamber is baked by an infrared lamp located inside the chamber. Target evaporation is effected by an excimer laser. The chamber incorporates a PID feedback-controlled substrate heater capable of reaching temperatures of up to 1,000 C and maintaining them accurately. Using this technique we have been able to obtain KTO, KNO, SBN thin films.

SBN thin films were prepared by reactive PLD. The stainless steel chamber used for this work is evacuated by a turbomolecular pump. A mass flow controller regulates gas admission for reactive PLD growth. The laser source is an excimer laser (Lambda Physik Compex 110) operating at 248 nm (KrF excimer) with a maximum repetition rate of 100 pulses per second. Beam incidence is ~45° onto rotating $Sr_xBa_{1-x}Nb_2O_6$ targets. Composition x = 0.61 was fabricated by cold-pressing and subsequent sintering of SBN powders previously obtained from solid state reaction of high purity $SrCO_3$, $BaCO_2$, and Nb_2O_3 powders. Film samples were grown on fused quartz substrates. The films appeared smooth and clear, with optical interference fringes due to thickness variation typical in PLD. The other thin film samples of supperlattice were obtained through the collaboration with the DoE Lab using the same PLD technology. A superlattice with excellent crystalline quality and consisting of alternating layers of paraelectric $KTaO_3$ and ferroelectric $KNbO_3$ (KNO/KTO supperlattice) was grown on a $KTaO_3$ (001) substrate by PLD. The lattice mismatch is less than 0.5%. The alternating $KNbO_3$ and $KTaO_3$ films were grown using a KrF excimer (λ = 248nm) laser as a light source. The superlattice consists of a total of 8 layers with thicknesses of 40 nm ($KTaO_3$) and 30 nm ($KNbO_3$).

2) Display materials - Eu^{2+} activated phosphors

We developed several new phosphorous materials including the red phosphor

$CaAl_4O_7:Eu^{3+}$, the blue phosphor $SrAl_4O_7:Eu^{2+}$, and persistent green phosphor $SrAl_2O_4:Eu^{2+}$, Dy^{3+}.

The first excited state of Eu^{2+} in some host materials can be a mixed state with electronic configuration $4f^65d^1$. The transition from the ground state $^8S_{7/2}$ to the 4f5d state is an inter-configuration transition and can be both electric dipole and spin allowed. Due to strong coupling with lattice, the absorption transition can span entire UV band A and band B. Large Stokes shift can provide fluorescence from ultra violet to red depending on hosts. Divalent Eu ions are attractive to energy efficient phosphors.

Thin films were prepared by spinning technique. The fresh wet gel was dropped onto a glass or quartz substrate which was spinning on a spin coating machine. The thickness of the thin films can be controlled by adjusting spin speed. The thickness of the thin films of $Eu:SiO_2$ prepared in this work is estimated to be about 700 nm. The dry glasses and thin films were annealed at temperature 400 to 800 °C for 4 hours. The raising rate of the annealing temperature was less than 30 °C per hour in order to get crack-free samples. Both bulk samples and thin films were amorphous. X-ray diffraction spectrum of the sol-gel glass SiO_2 is a structureless broad peak. Similar result was obtained from the thin film samples.

3)Porous sol-gel glass

Trivalent europium ions and transition metal ions Cr^{5+} doped in SiO_2 sol-gel glasses has been continued. Europium-doped materials are important luminophore for lighting and display. Sol-gel technology has been well developed by chemists, providing a unique way to obtain homogeneous composition distribution and uniform doping, and the processing temperature can be very low. In this work, Eu^{3+} doped SiO_2 thin films and glasses were prepared by sol-gel technology and their spectroscopic properties were investigated.

Eu^{3+}-doped SiO_2 thin films and glasses were prepared by sol-gel technology. Starting materials were tetraethoxysilane (TEOS = $Si(OEt)_4$), ethanol and water with the molar ratio 2:1:1. Drops of HCl acid was added as catalysis into the mixture to adjust its pH value to ~ 3.5. The

mixture was stirred using an ultrasonic stirring machine. Meantime, adding certain amount of the aqueous solution of $EuCl_3$ dropwise to a required doping level (2 wt% Eu based on SiO_2). Wet gels were obtained by hydrolysis process of the alkoxide. For bulk samples, the obtained wet gel was dried slowly at 45 °C in air in a plastic curvet sealed with parafilm having a pin hole on it for about two weeks. Clear transparent SiO_2 dry gels were obtained. Optical properties of nanoparticles materials have been studied extensively in recent years. These materials behave differently from bulk semiconductors and have stimulated great interests both in basic and applied researches. Chromium ions are very attractive to optical spectroscopy and laser physics. It is well known that the first laser in the history is a ruby laser activated with Cr^{3+}.[7] It was found in early nineties that Cr^{4+} was also an interesting lasing ion in the near infrared,[8] and various Cr^{4+} lasers have been developed.[9] Very recently, it was reported that Cr^{2+} doped in CdSe crystals showed lasing action in the infrared.[10] The above achievement have stimulated an interest in searching for Cr^{5+} and investigating its optical properties.

Cr^{5+} is isoelectronic with Ti^{3+} and V^{4+}, having electron configuration $3d^1$. Ti^{3+} is the active center of commercial cw and femtosecond sapphire lasers, tunable in the range 680-1100 nm. V^{4+} doped in $YAlO_3$ and Al_2O_3 showed broad band emission near 635 nm.[11] Although EPR results of Cr^{5+} were reported,[12,13] the optical properties were less studied. Herren et al. reported an observation of luminescence from Cr doped in SiO_2 sol-gel glass.[14,15] The luminescence spectrum was assigned to pentavalent ions in their first paper,[14] and later it was identified to be the emission from the charge transfer transition of Cr^{6+}.[15] The first observation of photoluminescence from octahedrally coordinated Cr^{5+} in BaCaMg aluminate glasses was reported very recently.[16]

In our research, we find luminescence results of Cr doped SiO_2 sol-gel glasses. The fluorescence spectra are very different from Herrens' results, and we believe it originates from pentavalent Cr.

Cr-doped SiO_2 glasses were prepared by sol-gel technology.[17] Starting material is

tetraethoxysilane (TEOS = $Si(OEt)_4$) doped with 0.2wt% Cr (based on SiO_2) in the isopropanol solution of $Cr(OOC_8H_{15})(OC_3H_7)_2$. Wet gels were obtained by hydrolysis of the alkoxides. The molar ratio of TEOS, ethanol and water (pH ~ 3.5) for hydrolysis was 2:1:1. The obtained wet gel was dried slowly at 45 °C in air in a plastic curvet sealed with parafilm having a pin hole on it for about two weeks. Clear transparent SiO_2 dry gels were obtained. Cr doped samples show blue-green color indicating the existence of Cr^{3+}. The dry glasses were annealed at temperature 400 to 800 °C for 4 hours. It seems that Cr ions in SiO_2 dry gels are easy to be oxidized. Cr doped samples turned to yellow after annealing above 400 °C in air.

II. NONLINEAR OPTICAL SPECTROSCOPIC STUDIES ON PLD THIN FILMS

1)SBN thin films

The mixed-crystal family $Sr_xBa_{1-x}Nb_2O_6$ (SBN) is one of the most important photorefractive materials. It exhibits an exceptionally large diagonal electro-optic (E-O) coefficient r_{33} compared to all E-O crystals reported to date, and therefore has a strong potential for applications in optical data storage, switching and optical computing. On the other hand, the trivalent Eu^{3+} ions doped solid state materials have received special interest among those incorporating rare-earth ions. This is not only due to the sensitive Eu^{3+} ions, which can be used as a structure probe, but also due to its large quadrupole splitting and spin-lattice relaxation times which make Eu^{3+} particularly attractive in high-resolution laser spectroscopy [18]. The practical importance of such a system lies in the promising application, currently proposed for a frequency domain optical data memory based on its large ratio of inhomogeneous-to-homogeneous line widths. In Y_2SiO_5 crystal Eu^{3+}shows the longest ever dephasing time of 822μs by photon echo experiment, and the narrowest homogeneous line width by hole-burning experiment in solid state materials, at low temperature, were observed [19]. This has stimulated interest in searching for appropriate materials to host Eu^{3+} ions, which could be optimized for operation at room temperature. This would represent a revolutionary advent in

information storage application.

A. Ultrafast nonlinear optical response

Ultrafast nonlinear optical response of the samples was measured in a picosecond-DFWM experiment using a ps Nd:YAG laser as pump source. The output wavelength was set at 560nm. The difference in index of refraction between substrate and film is about 0.46, which could bring into question sensitivity problems.

Fig. 1 shows the normalized diffraction signal intensity as a NLO response versus probe pulse delay at a ±250 psec region in the DFWM measurement for an undoped amorphous SBN thin film sample with thickness of ~ 0.5 μm (solid line), a bare fused quartz substrate (dash-dot line)

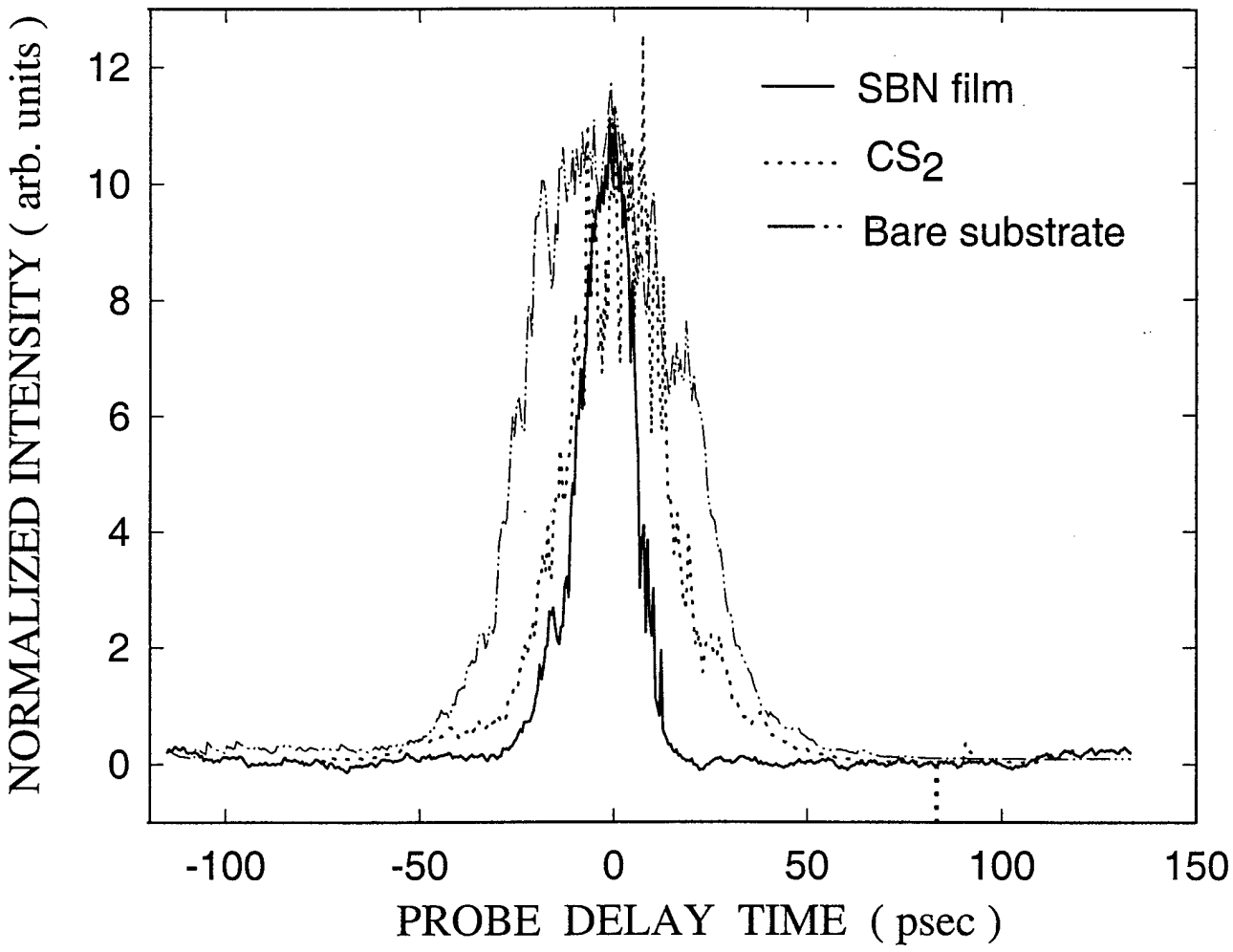

Fig.1 DFWM spectra of SBN thin film

identical to the one used for film deposition and the CS_2 reference (dotted line). For the thin film sample the laser intensity was typically 60 mJ/cm^2 while it was 30 mJ/cm^2 for CS_2 and 100 mJ/cm^2 for the bare substrate. Within a 500ps time scale only an instantaneous nonlinear optical response signal at zero delay of probe pulse could be observed, as shown in the figure. This transient response signal is associated with the third-order susceptibility $\chi^{(3)}$ of the measured material. The signal width of the instantaneous optical response is supposed to be equal to the autocorrelation width (~35 psec) of the three pulses if no additional mechanism contributes to the width. In the thin film measurement two interesting features were observed. First, a significant enhancement of $\chi^{(3)}$ with respect to bulk values was found. The value of $\chi^{(3)}$ is estimated to increase by 2 orders of magnitude in transverse alignment. Second, a significant squeezing of the coherent response signal was noticed. As shown in the figure the FWHM of the SBN film is 30% and 70% narrower that that of CS_2 standard and bare substrate of fused quartz, respectively. As verified experimentally, the laser beam intensity used in this measurement was not sufficient to cause TPA in bulk SBN crystal. However, TPA probably cannot be ruled out for the thin film. The intrinsic nonlinear optical response signal generated in this circumstance can be analyzed as the probe beam diffracted by the grating formed by the two pump pulses, A and B, which intersect at an angle of 2θ inside the thin film. The grating vector is $\boldsymbol{q} = \pm (\boldsymbol{k}_A - \boldsymbol{k}_B)$ confined in the film along x direction. The electric field amplitude A is therefore equal to $A_A e^{+ikx} + A_B e^{-ikx}$, where k represents the wavevector. Since the polarizations of A_A and A_B are identical (ss) in this experimental setup, the light intensity modulation is thus $I = I_A + I_B + 2\Delta I \cos(2kx)$, where $\Delta I = 1/2 n \epsilon_0 A_A \cdot A_B$. In our experiment $I_A = I_B$, so $I = 2I_A[1+\cos(qx)]$ for polarizations (ss). The diffracted signal intensity is directly related to the third-order susceptibility [20] by $\eta = \exp(-\alpha d/\cos\theta)\sin^2(d\pi\Delta n/\lambda\cos\theta)$, where $\Delta n = (12\pi/n_0\langle E^2\rangle)\chi^{(3)}$, E is the optical electric field, equal to $(8\pi/cn_0)F$, and F is the laser fluence. d stands for grating thickness, which equals the film thickness in this case. For homogeneously amorphous thin films, $\chi_{ssss} = \chi_{pppp}$ or $\chi_{iiii} = \chi_{jjjj}$, χ_{spps} and χ_{pssp} are independent. From the absolute diffraction efficiency measurements, we obtained $\chi_{1111} = \chi_{2222} = \chi_{3333} = 2.6 \times 10^{-11}$ esu.

The second feature observed in NLO response of SBN film is a "squeezing" effect. We previously noticed this kind of effect in perovskite crystals of $KNbO_3$ and KTN, and reported it as compression effect of the DFWM signal in bulk crystal [21]. The narrowed signal was shifted towards negative delay. It was identified as due to TPA interaction between the pump and probe pulses when the laser fluence was greater than 280 mJ/cm^2. In the present case, however, the laser fluence was lower and the peak does not shift apparently. Further increasing the laser power would, unfortunately, cause the film to be damaged. For the quartz substrate, on the other hand, a broadening was observed when increased laser power was employed (Fig.1). In this case TPA will produce free carriers in the conduction band, followed by radiationless relaxation with a large number of nonequilibrium phonons launched. The observed broadening in the substrate material actually originates from the scattering by long-lived phonons.

B. Luminescence of undoped and Eu^{3+}-doped thin film

It is generally more difficult to measure the absorption spectrum of thin films with thicknesses less than 0.5 μm unless a significant absorbance exists. For Eu^{3+}-doped SBN thin film the f-f optical transition due to europium dopant is Laporte forbidden, leading to very weak absorption. Thus no absorption due to Eu^{3+} ions was measurable. Instead, an intense charge transfer band at UV region with a cut-off-edge at ~343nm was observed. From bulk SBN crystal to thin film a blue shift was reported, but not fully understood according to the literature [22]. We believe that the blue-shift observed in the thin film is due to the internal stresses existing in the films, which originates from the lattice mismatch as well as the thermal expansion difference between the film and the substrate. The consequence of this stress is to cause the band gap to increase. The absorption edge actually corresponds to the intrinsic interband transition between the valence band, which consists of $p\pi$ orbitals of the oxygen electrons in this case, and the conduction band, which consists of $d\xi$ orbitals of Nb electrons. The gap was found to be increased by nearly 0.9 eV from bulk sample to the thin film. A broad but weak emission with FWHM of 3000 cm^{-1} was observed

when excited at 355 nm by the third harmonic of a Nd:YAG laser. The band maximum is at at 500nm. Cooling the sample down from room temperature to 7 K does not produce any distinct shift in band maximum. The lifetime was also measured and found to be ~10-20ns, close to the data obtained for bulk SBN crystal. The mechanism of this emission can be recognized as originating from excitons, and interpreted as follows. With the laser excitation, charge carriers can be produced in the conduction band. These will be trapped at the central niobium center to form quadravalent Nb^{4+}, leaving holes behind in the valence band.

Eu^{3+}-doped SBN thin film shows a typical amorphous nature in fluorescence measurement. Using UV excitation at 355 nm the emission profile consists of two broad features. One is peaked at 500 nm which belongs to the exciton emission while the other is peaked at ~610 nm with some weak components showing at ~700 nm. The f - f transition to multiplets of the ground state in unannealed film is not well resolved even at 4 K. Using excitation at 526 nm (corresponding to $^7F_0$ - $^5D_1$ transition), $^5D_0$ is populated. In this case the exciton emission is eliminated, leaving several broad components attributed to Eu^{3+}. The main emission at 4K is peaked at 613 nm with a shoulder at the low energy side. This can be assigned to $^5D_0$ - $^7F_2$ transition with the shoulder assigned to the j multiplets. $^7F_0$ and $^7F_1$ components are merged as a onebroad band while $^7F_3$ and $^7F_4$ components are resolved though the intensities are weak.

The annealed Eu^{3+}-doped SBN sample shows a typical crystalline feature. All Stark components of $^5D_0$ - ^{7}Fj transition were well resolved at low temperature of 4 K. For transition $^5D_0$ - $^7F_0$ there is only a single line obtained. The linewidth is 18 cm^{-1}, which is broad compared with that of other Eu^{3+}-doped single crystals. For transition to $^7F_1$, three components, and for $^7F_2$ five components were observed.

Crystallographic studies by Neurgaonkar et al [23] have shown that with strontium content x=0.61 the tetragonal SBN has a tungsten-bronze composition with chemical formula $(A_1)_4(A_2)_2C_4B_{10}O_{30}$ or $(A_1)_4(A_2)B_{10}O_{30}$, in which A_1, A_2, C, and B are 15-, 12-, 9-, and 6-fold coordinated sites, respectively. The 15- and 12-fold coordinated sites are partially empty in this

system. In previous study on Ce^{3+} singly doped and Ce^{3+}-codoped SBN, Ce^{3+} ions were found to occupy either in a 15-, 12-, 9-fold or a 6-fold cage [23]. According to this conclusion, in Eu^{3+}-doped SBN, Eu^{3+} seems to be able to situate also in either coordinated site. From the emission spectral measurements, however, only one set of $^5D_0$ - ^7Fj transitions was observed. Among them a single line of $^5D_0$ - $^7F_0$ transition with inhomogeneous linewidth 18 cm^{-1} is at ~ 577.3 nm. Therefore, Eu^{3+} ions can only occupy one site in SBN thin film. Comparing the ionic radii, where Eu^{3+}:0.95 Å; Ce^{3+}:1.03 Å; Sr^{2+}:1.12 Å and Nb^{5+}: 0.69 Å, Eu^{3+} is likely to fill the empty sites with a loose coordinate structure. However, the Stark component splitting, particularly the total energy level splitting of the $^7F_1$ state (~305 cm^{-1}) in the annealed film indicates that the crystal field is rather strong in this sample. In other words, the ionic bonding between Eu^{3+} and oxygen ligands seems to be stronger, with some covalency character. Based on this consideration Eu^{3+} ions are most likely to substitute Nb^{5+} in the 6-fold coordinate sites. In this case a negatively charged oxygen ion is necessarily moved away for charge compensation. This consideration may result in lowering the symmetry of Eu^{3+} sites to almost C_s. The theoretical calculation of energy levels might not give the further insight since for accurate calculation of C_s symmetry, 14 independent crystal field parameters are needed to compose the crystal field Hamiltonian. Based on the assumption of this symmetry, all energy levels including their multicomponents are assigned experimentally. Among all transitions, the electric dipole transition (absence of inversion) to $^7F_2$ is strongest in this sample while the magnetic dipole transition to $^7F_1$ is also clearly strong.

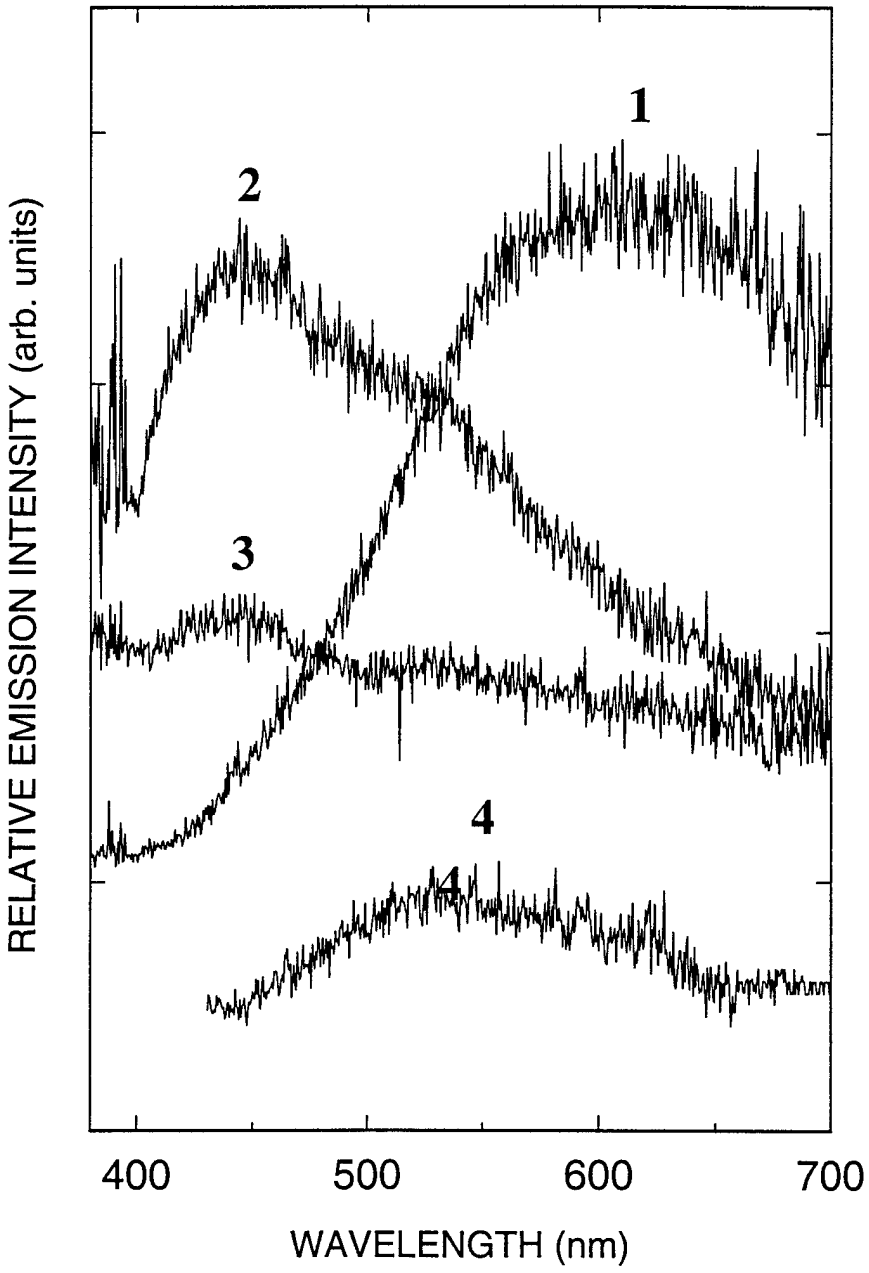

Figure 2. Fluorescence of (1) $KNbO_3$, (2) $KTa_{0.98}Nb_{0.02}O_3$, (3) $KTa_{0.78}Nb_{022}O_3$, (4)$KTaO_3$ at room temperature

2) Alternating films of KT/KTN

The ABO_3 incipient perovskite-like ferroelectrics with off-center impurities, namely, $KTaO_3$ (KTO) with Li, Nb, Na impurities, are of interest at least more than last twenty years. It connects with the appearance of impurity induced ferroelectric phase transition as well as glass-like states controlled by impurity concentration. It is especially characteristic for KTO:Nb (KTN) that the previously developed "single off-center impurities correlation" model can not be so effective in comparison with another type of actual model in this situation. Another important aspect of the perovskite-like oxygen-octahedral ferroelectrics is that the light-induced excitations may be responsible for the change in refractive index. Potassium tantalate and potassium niobate are of particular interest among the perovskite-structure ABO_3 materials because their para- or ferroelectric properties can be drastically altered by small changes in structure introduced either mechanically, by stress or chemically, by introducing other ions. Pure $KTaO_3$ is a cubic-symmetry crystal with a mean B-O distance of $a = 1.99$ Å, which is always in the paraelectric phase at room temperature or above. By contrast, pure $KNbO_3$ changes its phase from cubic (O_h $Pm3m$) into tetragonal (C_{4v} $P4mm$) at 704 K, and into orthorhombic (C_{2v} $Amm2$) at 498 K, and finally becomes rhombohedral (C_{3v} $R3m$) with a mean B-O distance of 2.85 Å at 265 K in a ferroelectric phase. We have studied the PLD-grow $KNbO_3/KTaO_3$ (KN/KT) superlattice which consists of alternating layers of paraelectric $KTaO_3$ and ferroelectric $KNbO_3$ grown on a $KTaO_3$ (001) substrate. Fig.2 and 3 represent the fluorescence spectra of the bulk crystals - potassium tantalate, potassium niobate, KTN and the KN/KT superlattice. Figure1 shows that all samples exhibit broad luminescence in the visible region. In the pure KTO_3 crystal, the emission was found to be weaker compared to the other samples. Its emission maximum is at 550 nm with a band width of ~6000 cm^{-1} covering 400 through 700 nm spectral range. The spectral profile of the pure KTO_3 does not vary with changing

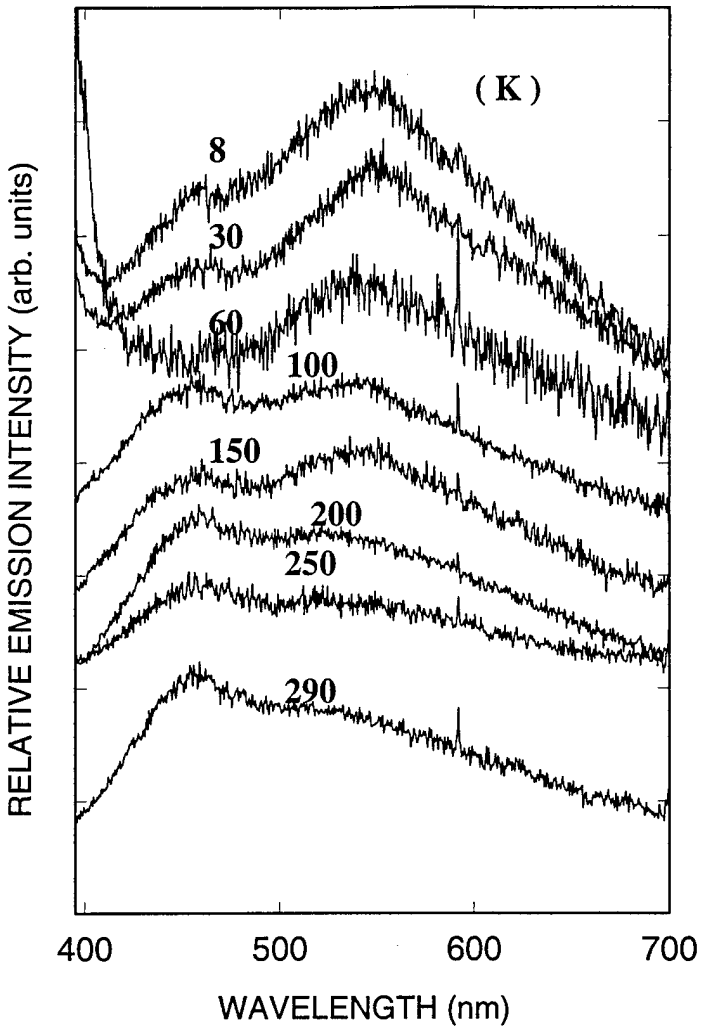

Figure 3.Temperature dependent fluorescence spectra of superlattice

temperature from 8 K till room temperature. In the pure $KNbO_3$ crystal, however, the emission was found to be stronger. The band maximum is at 610 nm with a band width of 6300 cm^{-1}. In ABO_3 incipient perovskite-like ferroelectrics with off-center impurities, such as Nb, the charge transfer vibronic excitons (CTVE) induced by one-photon or two-photon absorption of ferroelectric solid solution $KTa_{1-x}Nb_xO_3$ is considered as an origin of the transient optical response. The CTVE are created by charge transfer between oxygen and tantalum, or oxygen and niobium ions with appearance of O- - Ta^{4+} or O- - Nb^{4+} pairs accompanied by self-consistent lattice distortion. This lattice distortion is caused mainly by strengthening of the vibronic interaction in final recharged ion

states of CTVE. Dipole - soft TO-phonon interaction as well as Jahn-Teller type of interactions are effective. Due to a strong interaction of central B ions with lattice oxygen atoms, the emission of CTVE associated with O- - Ta^{4+} is supposed to be much weaker than that of O- - Nb^{4+} and both should decay fast. The creation of two-peak like emission either in KTN or in the KN/KT superlattice is presumably attributed to Ta^{4+} -- O- - Nb^{4+}, a new type of mixed CTVE.

The NLO response of the superlattice was also characterized using DFWM technique. The pump-pulse intensity was typically 30 - 50 mJ/cm^2. Within 500ps time scale, all samples show an instantaneous nonlinearoptical response with a half width of about 35 psec located at zero delay of the probe pulse. A significant enhancement of $\chi^{(3)}$ was found for the superlattice film. The value of $\chi^{(3)}$ which is evaluated by calculating the coherent signal intensity was found to be, in comparison with the bulk sample, increased by 2 orders of magnitude in transverse configuration. The DFWM signal of the $KTaO_3$ substrate and the KN/KT superlattice shows a significant enhancement of $\chi^{(3)}$. The value of $\chi^{(3)}$ was obtained as follows: for a $KTaO_3$ substrate : $\chi_{1111} = \chi_{2222} = \chi_{3333} = 0.32 \times 10^{-13}$ cm^3 erg; for KN/KT superlattice thin film: $\chi = 0.93 \times 10^{-11}$ cm^3 erg.

3) The influence of the internal photo-induced electric field on the formation of self-pumped phase conjugation in doped KNSBN crystals

In the past decade, high phase-conjugate reflectivity has been obtained in the simplest and most elegant total internal reflection self-pumped phase conjugators(SPPCs) in photorefractive (PR) crystals of $BaTiO_3$ [24,25] and $(K_xNa_{1-x})_a(Sr_yBa_{1-y})_bNb_2O_6$ (KNSBN) [26,27]. This kind of SPPC was first demonstrated by Feinberg [28] and sometimes was also referred as CAT SPPC by others. Although the SPPC possesses some intrinsic advantages of structure simplicity, relative insensitivity to vibration, self-alignment, etc., its slower response rate impedes its applications in an extensive domain. It is very important to find a way in which the response rate can be raised. Thermal gratings and the influence of pyroelectric (PY) effect on the PR process draw great attention

recently [29-35]. In tungsten bronze family crystals of $Sr_xBa_{1-x}Nb_2O_6$ (SBN) and KNSBN, the photo-induced field stemming from photovoltaic (PV) effect and PY effect was investigated previously.[26,33] Yet little attention to our knowledge was paid to the influence of this kind of field on formation of self-pumped phase conjugation in these crystals. In our experiment, an Ar^+-laser beam was divided into two-parts by a beam splitter BS. Then the unfocused beam polarized in the plane of the paper (extraordinary to the crystal) illuminated a single-domain doped KNSBN crystal. A shutter S was inserted in the path to control the illuminating mode on the crystal. The returning phase conjugate beam was monitored with a photodiode D_1. An iris diagram placed in the input path was used to control the incident beam size. The crystal was mounted on a platform allowing the controlled rotation and horizontal displacement so that the effect of the beam input position (X) and incident angle (θ) were precisely adjustable. KNSBN samples were cut as: 6.4mm×6.0mm×4.2mm for Ce:KNSBN with 0.01wt.% Ce sample 1, 8.4mm×5.1mm×6.1mm for Mn:KNSBN with 0.05wt.% Mn sample 2; and 6.4mm×5.5mm×5.2mm for Cu:KNSBN with 0.03wt.% Cu sample 3; respectively.

A curious appearance of the returning phase conjugate output was observed when the laser beam (power 12.2mW, diameter 2.0mm) at 514.5nm was incident on the sample at incident angle of θ=42.5° and incident position X=2.0mm. It was found if a cw illuminating mode was used, no output could be monitored on D_1 within 1000 seconds. However, if the laser beam with intermittent illuminating mode impinged on the crystal, returning phase conjugate output could be received on D_1 within an interval less than 24 seconds. Similar experimental results of self-restrained effect were also observed in sample 1 with the laser wavelengths at 632.8, 496.5 and 488.0nm, respectively. When a laser beam of He-Ne laser at 632.8nm was incident onto the sample 1, the interval in which the laser beam was blocked should be longer than that of Ar^+ laser at 514.5nm (at the same incident powers). The dwelling interval should be 30 to 250S under some situations.

It is well known that in a PR crystal the charge transfer may occur as diffusion due to non-uniform free carrier distribution, or as drift in external field and in space charge field, or as moving from internal PV effect. For KNSBN crystals, the introduction of some trace of dopants (such as

Fe, Ce, Cu, Mn, etc.) may dramatically strengthen their PV effect. According to Carrascoca et al's work[14], the PV effect can be simplified as it is equal to the applied field. The net current density for monochromatic excitation along the polar z-axis is then given [34] as

Where μ is the charge carrier mobility, n the free charge concentration, k_B the Boltzmann's constant, T the absolute temperature, E_{sc} the space-charge field component along the z-axis, E_0 the externally applied field, E_{pv} the PV field stemming from preferably moving of the liberated charge carriers in one direction,

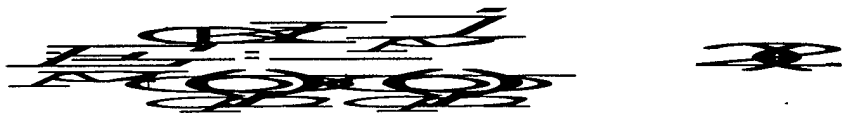

Where j_{pv} is the current density corresponding to PV effect, σ_d and σ_{ph} are the dark conductivity and photoconductivity respectively, α the absorption coefficient, I the incident intensity, κ the PV constant proposed by Glass et al.[36] For PY crystals, the contribution of the PY effect to the current can not be neglected in case where the illumination is altered. This contribution is equivalent to an electric field along the negative polar axis.

When a sinusoidal interference pattern $I = I_0 + I_1 \sin Kz$ (with $I_0 >> I_1$) produced by two crossing light beams illuminates on a PR crystal, a grating with grating vector $K=2\pi/\Lambda$, period of grating $\Lambda=\lambda/2n_0\sin\theta$ is formed inside the sample. The steady-state space charge field can be experessed in our experiment[15]

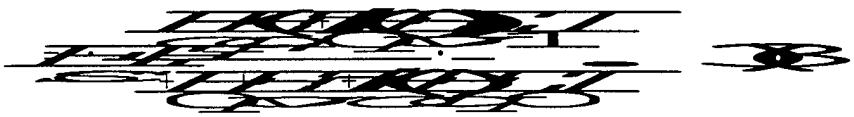

with F a constant for a given crystal. $E_d=k_BTK/e$ is diffusion field, $E_q=N_Ae/\epsilon\epsilon_0K$, N_A is the trapped

site concentration, ϵ_0, ϵ permitivity for free space and medium.

The asymmetry of the drift leads to a spatial phase shift ϕ between the produced grating and the interference pattern. The phase shift ϕ can be easily obtained from Eq. (3)

The optimal state of energy transfer corresponds to $\phi = \pi/2$. The phase shift ϕ shows great influence on the beam coupling in PR crystals. One can see from Eq. (4) that deviation from the optimal energy coupling could come up as a result of nonzero value of the sum of E_0+E_{pv} if no other action is exerted on the electric carrier migration.

In the case of an applied field, the phase coupling between the beams should take place. According to the Kukhtarev-Vineskii model, one obtains phase variation for one of the optical waves in the co-directional two-wave-mixing configuration[18]

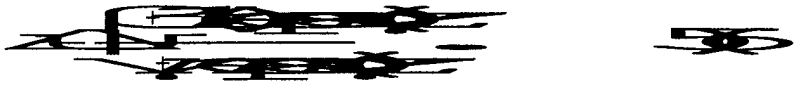

Where $\gamma=2\pi n_1 \sin\phi/\lambda\cos(\theta/2)$ is the intensity gain factor, $\beta=\lambda n_1\cos\phi/\lambda\cos(\theta/2)$ the phase conversion factor, $\beta/\gamma=\cot\phi/2$, $m=I_1(0)/I_2(0)$ the input intensity ratio, n_1 the first Fourier component of the photo-induced refractive index distribution, and θ the crossing angle of the two beams.

It should be pointed out that the above analysis is based on steady state. For a transient state, the electric field stemming from PY effect may play an important role for the charge migration, in other words, the PY field can be equivalent to the applied field.

In doped KNSBN crystals, the relationships between the photocurrent density and the applied dc field E_0 under different incident light intensity I were obtained, showing some clues of the

effective PV field. A halogen-tungsten lamp and a Pico-ampere galvanometer were used in the measurement. The effective PV field could be calculated from Eq. (2) if the value of j_{pv} corresponding to $E_0=0$ and values of the dark conductivity and photoconductivity σ_d and σ_{ph} were obtained. We obtained $\sigma_d < 10^{-13}\Omega^{-1}cm^{-1}$, and $\sigma_{ph}=1.0\times10^{-12}\Omega^{-1}cm^{-1}$, then~ $7.8\times10^3 V.cm^{-1}$ PV field could be calculated. Once again one can see from Eq. (1) that PV field and applied field are only two factors which may drive the macroscopic current. When the applied field is just as great as PV field, the derived current equal zero. Thus the effective PV field can be estimated by extrapolating the fitting curve of the photocurrent density vs applied field. It was found to be $8.0\times10^3 V.cm^{-1}$, $2.7\times10^3 V.cm^{-1}$, $0.8\times10^3 V.cm^{-1}$, and zero respectively for sample 1, 2, 3 and the nominally pure KNSBN crystal.

This effective PV field may drive the charge carriers to move toward one direction in the crystal. Therefore the optimal energy coupling (corresponding to $\phi=\pi/2$) could not be realized for a cw mode.

4) Investigation into self-pumped and mutually-pumped phase conjugation with beams entering the negative C-face of Cu-doped KNSBN crystals

Self-pumped phase conjugator (SPPC) basing on total internal reflection (TIR) from the crystal corner was well studied, a variety of compact SPPC and mutually-pumped phase conjugation (MPPC) geometries have also been demonstrated. In Cu-doped KNSBN (Cu:KNSBN) crystals a few papers about MPPC with KNSBN have been published to our knowledge. In our experiment , SPPC based on both reflection from a-face and TIR from the corners of the Cu:KNSBN crystals isstudied with a beam entering negative c-face. A novel MPPC with hawk-beak-like configuration was demonstrated in the same samples for the first time to our knowledge. We observed different internal light paths and their direct transformation only via varying the incident position and incident angle. These observations may give a deeper insight into the mechanism of the SPPC and MPPC in doped KNSBN and may enrich the knowledge about the negative c-face-entering geometries. A

monochromatic light beam from an argon-ion laser operating at 514.5nm was used as a light source. The incident beam was polarized and returning phase conjugate beam was monitored with photoelectric detector D. When a laser beam with fixed input power 38.0mW and fixed diameter 2.0mm impinges upon the negative c-face of the sample, the diameter of the laser beam inside varies with the variation of the incidence angle. The fanning beams toward a-face can be self-generated immediately. For different input position X and input angle θ, the steady state internal light channels show different appearances.The output dynamic features of this kind of SPPC were also observed experimentally. The stability of the output become worse when the backward scattering play role in the SPPC; second, the response rate of the SPPC basing on backward scattering is slower than SPPC basing on the internal total reflection; third, the decrease of the diameter of the incident beam could increase the response rate of SPPC in this novel geometry.

The similar experimental results were obtained at other argon-ion laser wavelengths such as 488.0nm, 496.5nm, and 476.5nm. The internal light path transformation could be realized in all these wavelengths. This kind of SPPC was realized with Ce-doped KNSBN (with 0.05wt% Ce doping and with the absorption coefficient at 514.5nm was α=5.46cm-1) and Co-doped KNSBN (with 0.05wt% Co doping and with the absorption coefficient at 514.5nm was $\alpha=1.45cm^{-1}$) crystals too. In Ce-doped KNSBN and Co-doped KNSBN crystals, with larger absorption coefficients, only semicircle-like loop could be formed.

To demonstrate conjugation fidelity of the self-pumped phase conjugator, a collimated beam from an argon-ion laser was directed through a binary transparency and focused with an f=300mm lens into the Cu:KNSBN crystal. The power of the incident beam was 4.0mW at the crystal. The crystal was in front of or behind of the focal point a little distance. When the distance between the focus and crystal was 30mm, the phase conjugate beam can be monitored within half a minute. An edge-enhancement image was observed first. A steady phase conjugate output of the input image could be obtained within three minutes. The experimental result about conjugation fidelity of the self-pumped phase conjugator. In this situation, θ=80°, X=7.0mm, R_c=28%. It can be seen that

the output image was distortion-free even with a severe phase aberrator placed between the beam splitter and the crystal, proving that the crystal was producing the phase-conjugate replica of the incident wave. The corresponding internal light paths shows that two corners play important roles then.

The stability of the output of the SPPC was bad at the initial stage. The oscillating state normally switched to a stable state after a short time.

Some important features can be drawn from the above observations.

(1) Bifurcations of light beams took place on the surface of the sample.

(2) Multi-step bifurcation generally existed in the light paths.

(3) The appearances of internal light paths were different under different incident ways.

In order to get a general understanding to the mechanism of SPPC in Cu:KNSBN crystal, the performances of self-pumped phase conjugator under the configurations with a beam entering a-face and b-face should be given in brief.

Difference between KNSBN and $BaTiO_3$, KTN

The internal paths in our SPS SPPC are different from those in $BaTiO_3$ and KTN crystals. After the SPPC formed in $BaTiO_3$ and KTN crystals, internal paths could contract up in a region near the incident surface. This may owe to strong energy coupling from straight forward transmitted beam to the backscattering beams. In our experiments, no similar phenomenon of internal path contraction was observed. The counterpropagating beams were always formed relying on the reflection from the surface and from corner. It may be concluded that whether the total reflection or backscattering play important roles in SPPC is determined by the kind of the crystal and fabricated way of the sample.

It should be pointed out emphatically that a pair of a-faces (on which the backward SPS takes place) are poorly polished. This may be the reason why the SPPC based on the backward SPS from a-face can be realized easily in this sample, whereas the most SPPC configurations in Cu:KNSBN crystals belong to TIR geometry. We also would like to point out that the light paths toward the

surface of the crystal always terminate at defects or dust particles adhered to the surface. All these observations seem to imply that a novel kind of SPPC with Cu:KNSBN crystal, in which only one entrance face need to be polished, may be protested. Some thorough investigations should give a good answer to this suggestion.

The initial instability of SPPC output based on backward SPS may be the result of contradirectional two-wave mixing. The larger absorption coefficient may be the reason why in a-face or negative c-face entering geometry the reflectivity is smaller than that in b-face entering geometry.

The larger absorption coefficient may be the reason in a-face or negative c-face entering geometry the reflectivity is smaller than that in b-face entering geometry.

III. NANOCOMPOSITE MATERIALS

It is well known that the small and indirect band gap of crystalline silicon (c-Si) is characterized by an extremely low quantum efficiency of luminescence while porous silicon (PSi), obtained by electrochemical etching of c-Si surfaces, yields extremely high photoluminescence (PL) efficiencies up to 10^{-1} in the visible range [36]. The origin of the PL has been the subject of many studies. We have studied the photodynamical process and Raman spectra of PSi. It was found that S-band luminescence comes from highly confined regions with a distribution of wire widths. Quantum confinement increases the emission energy and the oscillator strength of the radiative transition, decreasing the radiative lifetime. Therefore the most accepted luminescence mechanism at this time is associated with quantum confinement in the nc-Si formed in the PSi by the anodization process. The presence of ~3 nm size nanocrystallites is the size required by the confinement mechanisms to enlarge the band gap. On the other hand, there is interest in the changes of the size-sensitive optical properties due to the quantum confinement. The microstructure of the vitreous state exhibits short-range order within a c-Si core but long-range disorder. The wave vector and eigenfunction associated with an optical process are thus no longer valid due to the lack of periodicity of the structure. In PSi the network can be tailored within one size-category by using size-sensitive, fast selective excitation. This will reveal the associated optical properties of the material, such as photorefractive sensitivity, FWM signal polarization, appearance of ultrafast NLO responses, optical activity, etc.

1) Optical properties

The optical quality, free standing and highly photoluminescent PSi was obtained from both, p- and n-type Si wafers using electrochemical anodization of c-Si. The sample studied here was prepared from a boron doped Si wafer with (100) crystalline orientation and 0.5-1.5 Ωcm resistivity. The anodization current (200mA/cm^2) was applied in 280 steps of 0.8sec each and with resting

intervals of 1.4 sec between anodizations, such that a high-optical quality, free-standing porous film was obtained. The absorption measurement was found that a sharp cut-off absorption edge at the high energy side is located at ~ 410nm and the low energy side is at ~ 510 nm (shown in the inset of Figure 4) with a tail extended to 600 nm. At the wavelength greater than 510 nm the absorption becomes very weak, and at 633 nmn the absorption is negligible.

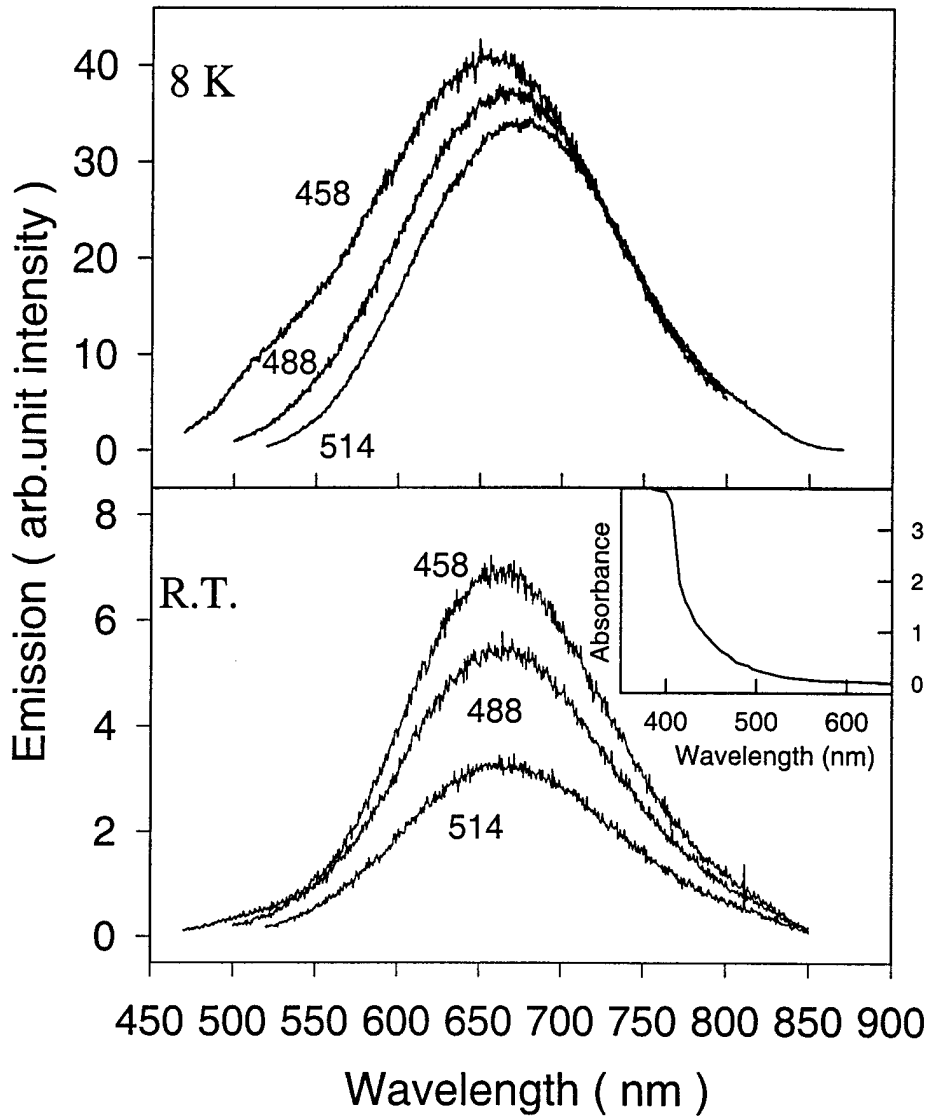

FIGURE 4. Emission spectra of PSi by excitation of an Ar^+ laser at 3 different wavelengths. The upper graph stands for low temperature at 8 K, while the lower one for room temperature. The inset represents represents the absorption spectrum.

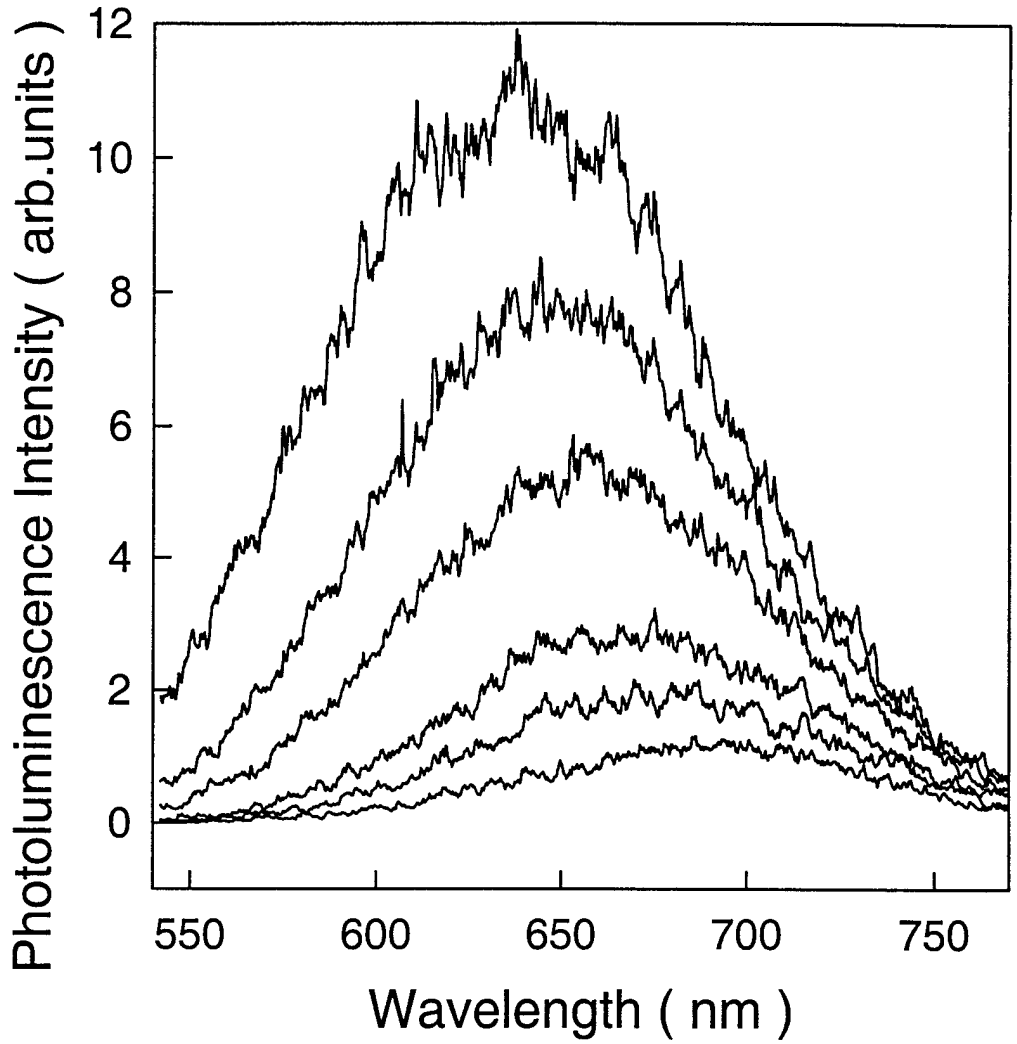

FIGURE 5. Time-resolved emissionspectra of PSi excited at 532 nm. The delay time from upper to lower:4, 24, 44, 64, 84 μs.

The emission measurements were conducted using lasers setting at different wavelengths covering

458 - 633 nm region in purpose to provide different excitation photon energy. Nevertheless, in all cases a broad band red luminescence can generally be observed. Fig.4 stands for a typical luminescence spectra of PSi at room and low temperature 8 K. Three lines from an Ar^+ laser at 458, 488 and 514 nm were used for excitation. At room temperature, the emission band maximum does not shift markedly with changing excitation wavelength, but emission intensity varies significantly because absorption changes from 458 nm to 514 nm. At low temperature 8 K however, the emission peak obviously shifts toward longer wavelengths while the excitation tuned to longer wavelength. But the emission intensity does not change so much as what observed at room temperature. It is presumably due to a flat plateau in this absorption region at low temperature. On the other hand, to compare the spectra obtained at different temperature no distinct correlation between peak position and temperature, or between emission bandwidth and temperature was observed. Furthermore, emission spectra excited at 633 nm.were also obtained, and used to compare with those excited at shorter wavelengths. The photon energy of 633 nm excitation is lower than the absorption edge 510 nm. However, the luminescence can still be observed. In all cases the common feature for all emission spectra is the large bandwidth. From excitation at 458 nm to 633 nm, the difference of bandwidth was found to be less than 10%. Therefore, it is suggested that all excitations are highly localized. Fig.2 shows the time-resolved emission spectra at room temperature. The excitation was at 532 nm with the delay time from 4 to 84μs. It features a typically glassy-like profile. As the delay time increases shorter-lived emitter dies out leaving luminescence due to longer-lived emitter dominant. As shown in the figure there is no interaction evidence in any emission profile. The contribution of phonon-assisted transition is less important here, compared to the case of 3d or 4f ions-doped materials The reason is two-fold, as discussed in the following. From general understanding we may assume two possible recombination processes. For those electrons excited from valence band to conduction band by excitation at 458 nm, they possess excitation energy well above the bandgap. A part of them could undergo a direct radiative transition in the area where they were excited while the others could migrate away. The

excitation migration would then be trapped in some different confined region, and emit from that region. If this latter case were true the entire emission would be an overlap of entire emission from different regions, resulting in a much broader and diffusive feature with an obvious wavelength dependence. On the other hand, for those electrons excited by 633nm excitation they possess energy well below the bandgap. These electrons can not undergo a migration process. They must immediately be localized and/or emit light from the excited region. In this case the emission profile is supposed to be not as broader as that in the former case. Therefore, because all emissions excited at different wavelengths exhibit similar breadth it implies that the confined regions giving light emission are mainly isolated and scattered in porous Si samples. This is in consistence with conclusions of other studies. For instance, the studies on the polarization of the luminescence of porous Si have supported the model that only limited migration of carriers to neighboring regions may occur [37,38]. The second-fold consideration is that in nanocrystals, the phonon spectra are modified due to the break-down of the lattice periodicity. Anharmonic effects of lattice vibration may also become important. A large number of activators are expected to be located in a distorted lattice environment near the surface. The radiative recombination in the localized state on the nanocrystallite surface causes the strong visible photoluminescence. This kind of PL is sensitive to the nanocrystallite size, and insensitive to the temperature.

2) Nonlinear optical properties

Study on nonlinear optical property of porous Si, particularly the transient optical response measurement has not yet reported to our knowledge. It is due mainly to the technical difficulty in performing such kind of measurements. With a green light source (available for most commercial pulsed lasers) the absorption by PSi film is too strong for the material to sustain. We are able to perform this kind of measurement by turning the picosecond light source into the yellow - orange region. using technique of picosecond optical parametric generation. A frequency-tripled $Y_3Al_5O_{12}$:Nd laser operated at 355 nm with pulse width of 45 ps was used for optical parametric

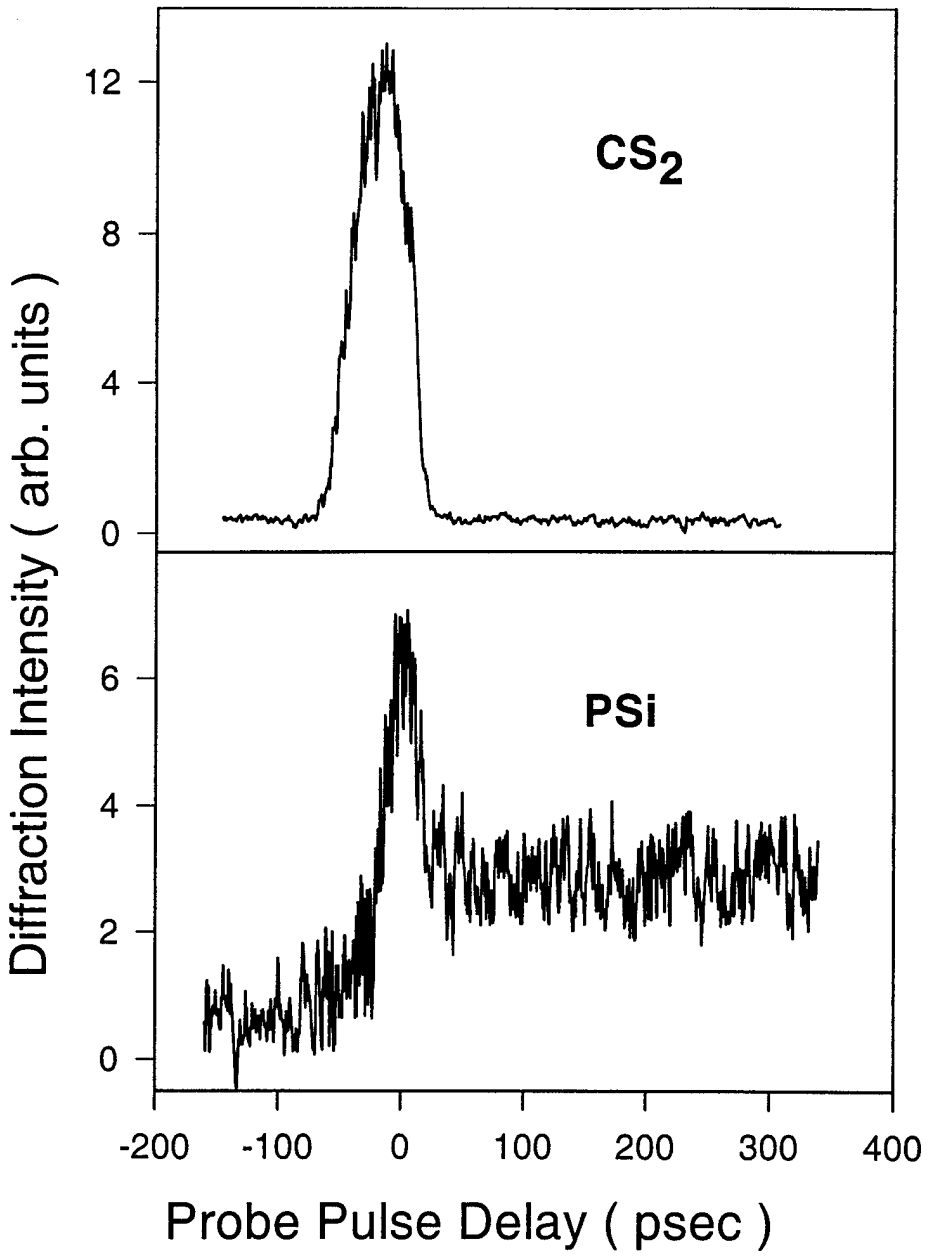

FIGURE 6. Picosecondnonlinear optical response of PSi compared with CS_2 reference.

generation. The output wavelength can be continuously tuned from 400 to 700 nm. In order to determine which wavelength can be best used for

characterization, the measurement was checked by turning laser was within 550 - 650 nm. Significant absorption by Psi free standing film in the region of 550 - 590 nm would cause a damage of sample. In the region of 590 - 600 nm the obtained response signal is dominant by the slow-response component which originates from the excited state population grating formed by the two pump-pulses across inside the sample. Tuning the wavelength beyond 610 nm caused the DFWM signal too weak to record in transverse geometry. The final measurement was therefore conducted at 604 nm. In the experiment the laser beam was split into two pump beams and a probe beam. The latter carried 10% of the total laser power. The probe went through an optical delay line, and was then incident on the sample from the substrate side. The two pump beams were crossed on the film at an angle, interfering to form a transient grating in the film. The delay line in one of the pump beam paths was used to ensure simultaneity of the pulses at the sample. The beam size of the probe was about 50% that of the pump. Thus, the probe could uniformly sense the susceptibility within the interference region of the two pump pulses. Fig. 6 shows the DFWM signal of free standing PSi wafer compared with CS_2 reference. For CS_2 reference, the intense coherent response signal with a half width of about 55 psec located at zero delay of the probe pulse is associated with the third-order nonlinearity of the CS_2 material. It is an instantaneous response. It comes from the change in polarizability of grating peak versus grating valley when 2 pump pulses are cross inside the sample writing a periodic bright-dark interference pattern. For CS_2 reference, the fast response is well know as due to the vibrational character of the intermolecular motion in liquid. The signal width is consistent with the intensity autocorrelation of the three laser pulses. For PSi sample, however, the signal consists of 2 components. The one is similar to CS_2, with the peak located at zero delay of the probe pulse. The other one is a slow response signal, can be identified as to start at ~ +30 ps of the probe pulse delay. The signal intensity of the slow response (SR) is almost a half of the instantaneous response signal, but it lives for much longer. By estimation it can enter into microseconds region.

The first component at zero delay is a direct measure of $\chi^{(3)}$ of the PSi material. It has two

distinct features. Firstly, the ratio of peak intensity to sample thickness is extremely large compared to most bulk crystals. In solid state materials the contribution to the instantaneous signal component may come from electronic cloud deformation as well as the nucleus reorientation. The latter contribution in solids is usually smaller. The second feature of the coherent response component is the squeezed nature in time domain. When the two pump pulses are polarized in the same direction, the coherent signal component is directly related to the third-order susceptibility by

$$\eta = \exp(-\alpha d/\cos\theta)\,\sin^2(d\pi\Delta n/\lambda\cos\theta), \tag{1}$$

where

$$\Delta n = \frac{12\pi}{n_0 \langle E^2 \rangle}\,\chi^{(3)}, \tag{2}$$

here, E *is* optical electric field, d is the grating thickness, and 2θ is the crossing angle of the two pump pulses. The intrinsic nonlinear optical response signal generated in this circumstance can be analyzed as the probe beam diffracted by the grating formed by the two pump pulses A and B, which intersect at an angle of 2θ inside the thin film. The grating vector is $\boldsymbol{q} = \pm(\boldsymbol{k}_A - \boldsymbol{k}_B)$, confined in the film along the x direction. The electric field amplitude A is

$$A = A_A e^{+ikx} + A_B e^{-ikx}, \tag{3}$$

where k represents the wavevector. The light intensity is then modulated as

$$I = I_A + I_B + 2\Delta I \cos(2kx), \tag{4}$$

here $\Delta I = 1/2n\epsilon_0 A_A \cdot A_B$. In our experiment, $I_A = I_B$, so $I = 2I_A(1+\cos(qx))$ for identical polarizations (ss) of A_A and A_B. The diffracted signal intensity is directly related to the third-order susceptibility as expressed by Eq.(1). Compare the FWHM of PSi sample to CS_2, the former is about 70% of the latter compared to the electronic part. For isotropic sample $\chi^{(3)}_{xxxx} = 3\,\chi^{(3)}_{xxyy} = 3\,\chi^{(3)}_{yxxy}$ [39]. We obtained $\chi^{(3)}_{xxxx} = \chi^{(3)}_{yyyy} = \chi^{(3)}_{zzzz} = 0.12 \times 10^{-11}$ cm^3 erg, which is significantly large compared to many bulk crystals.

3) Hot luminescence of Mn^{2+} in ZnS nanocrystals

Optical properties of semiconductor nanocrystals have been studied extensively in recent years. Because of the quantum confinement effect, a large ratio of surface to volume and the high density of surface states as well as the geometrical confinement of phonons, these materials behave differently from the bulk materials. It has therefore stimulated interest either in basic or in applied research. Our interest in the abnormal optical properties of Mn^{2+} doped ZnS nanocrystals was stimulated by observing an abnormal optical behavior of ZnS:Mn^{2+} nanocrystals and reported the irradiation-induced luminescence enhancement (IILE) effect of ZnS:Mn^{2+} nanocrystals in alcohol colloids and in polymer films. The abnormal temperature behavior of luminescence intensity of ZnS:Mn^{2+} nanocrystals in polymers was also studied.

The configurational coordinate model and Franck-Condon Principle have been successfully used to understand radiative and nonradiative transitions when a significant electron-phonon coupling is involved[40]. In these processes, electrons excited from the ground state of an optical center to the higher vibrational states of an excited state may relax to its lower vibrational states by emitting phonons, or relax to the electronic ground state by emitting photons. According to Franck-Condon principle, the most probable transitions from the excited state to the ground state should occur around the two classical turning points in the vibrational states of the excited state when the vibrational quantum number is not small. Consequently, two split-pair emission bands from the two turning points can be observed if these vibrational levels are highly excited. Although hot luminescence was studied in different materials, including materials doped with ions such as Cr, Cu and Ti[41], among which one of the authors has reported a hot-magnon sideband in the fluorescence spectrum of $CsMnCl_3.2D_2O$[42], the observation of two split-pair bands from the two classical turning points, however, has not yet, to our knowledge, been reported.

We report, for the first time, observation of two split-pair bands from the two classical turning points. It is a vivid manifestation of the configurational coordinate model. The time evolution of two bands may provide new information for study on electron and phonon relaxation in highly excited

vibrational states. The population and energy relaxation times of hot electrons in ZnS:Mn^{2+} nanocrystals were deduced.

Hot luminescence originates from transitions of electrons in higher vibrational states. It usually decays rapidly. However, many works have shown that a "hot spot" created under high excitation density can be extremely hot, resulting in enhanced phonon-phonon scattering which forms a long-lived phonon source with lifetimes in the order of microsecond range[43]. The long decay time of the hot luminescence of Mn^{2+} observed in our experiment is therefore assumed to come from such a " hot spot " which is localized by the nanocrystals.

Nanoparticles of ZnS: Mn^{2+} were made by the same method as described in our previous paper, Polyvinyl Butyral (PVB) was used as the polymer matrix. The concentration of Mn^{2+} is estimated to be less than 10^{-3} mol/mol ZnS.

A excimer pulsed laser was employed as the excitation source for measuring time resolved spectra. The excitation spectrum shows a significant blue-shift , which is ascribed to the well known quantum confinement effect. From this shift the size of ZnS: Mn^{2+} nanocrystals was estimated to be about 3.6 nm. Time resolved emission spectra show that there is no conventional Mn^{2+} emission band at short delay time. Instead, there are two split-pair bands with peaks at 540 nm and 660 nm. A dip is located at 590 nm, which is the peak position of the conventional Mn^{2+} emission band in ZnS. With an increase of the delay time, the splitting of two peaks decreases. The peaks at high and low energies shift towards 590 nm. A model proposed here is based on the Franck-Condon principle. A "hot spot" is formed in the excited region of the sample. The observed phenomenon is then a manifestation of hot luminescence from the classical turning points of the configuration coordinate curve of the $^4T_1$ excited state to the $^6A_1$ ground state of Mn^{2+} in ZnS. The electronic transition involving electron-phonon coupling can be understood in the frame of the well known configuration coordinate model and Franck-Condon principle. Under high excitation density, there are two emission bands peaking at the high and low energy sides of the peak position of the conventional emission band of Mn^{2+} in ZnS at short delay time. The peaks of these two bands shift

towards the peak position of the conventional band of Mn^{2+} in ZnS and merge into one band with increase of the delay time. These two bands are assumed to be hot luminescence, which comes from transitions from the two classical turning points of the high vibrational levels of the excited electronic state to the ground state of Mn^{2+} in ZnS. The long relaxation time (~μs) is caused by the formation of a " hot spot". The relaxation time increases with an increase of the excitation density, consistent with the expectation from the " hot spot " model. The population relaxation time t_p and energy relaxation time t_e of the hot electrons in the "hot spot" were deduced.

4) Charge generation and ultrafast NLO response in nanoparticle material

The VB - CB energy gap of c-Si nanoparticles is estimated to be ~ 3.0 ev [44]. Upon an intense laser excitation at 355 nm or by two photon absorption at 532 nm, photoinduced charge carriers are expected to be easily produced in CB. These carriers are moving around and might be trapped at some defect sites to form so-called shallow centers [45]. In order to understand the dynamical processes in the excited states, which is crucial for developing photofunctional materials, ultrafast and time-resolved degenerate four-wave mixing (DFWM) experiments were performed. A ps-Nd: YAG laser with OPG of pulse width 30 ps or a fs-laser system (Spectra-Physics Milliniam laser pumped Ti-Tsunami laser; Nd:YLF pumped Spitifier and fs-OPA) was used as the light source for obtaining time resolution in nanosecond or picosecond regime, respectively.

Fig.7 shows the optical response signal of samples versus probe pulse delay. The left part represents the ultrafast response of material in sub-picosecond scale while the right part represents the response in nanosecond region. In the figure, CS_2 and the quartz glass substrate are used for the references, in order for comparing each to others. It is clear that the obtained spectra of Eu^{3+} in c-Si/SiO_2 do not suffer any mechanical broadening other than the broadening due to photodynamic processes. The main feature of all profiles in the figure is an intense instantaneous response with the peak at zero delay time followed by a slow response (SR) due to transient gratings formed by pulsed laser beams crossing inside samples. The zero-delayed peak is associated with the intrinsic

third-order nonlinearity of the material, which is used to characterize the third-order nonlinearity of materials.

The characteristics of SR signals indicate that the transient population grating could be produced in both nanoparticle c-Si/SiO_2 and Eu-doped c-Si/SiO_2 samples but not in Eu-SiO_2. As shown in Fig.7, the right part, in nondoping nanoparticle c-Si/SiO_2 upon laser excitation the SR signal features an intensity buildup, reaching the maximum at the delay time of about 400ps. It decays slowly thereafter with a long-lasting tail extending out of the scale. In Eu^{3+}-doped nanoparticle c-Si/SiO_2 sample, however, this kind of alteration of the SR signal right after the instantaneous response was not observed. In the doped sample it features a slowly decaying signal with an average decay rate of 2 X 10^8/s, which corresponds to a half of the luminescence lifetime of nanoparticles (~10 ns as discussed above). It is interesting, and important to understand the physics behind based on these observations.

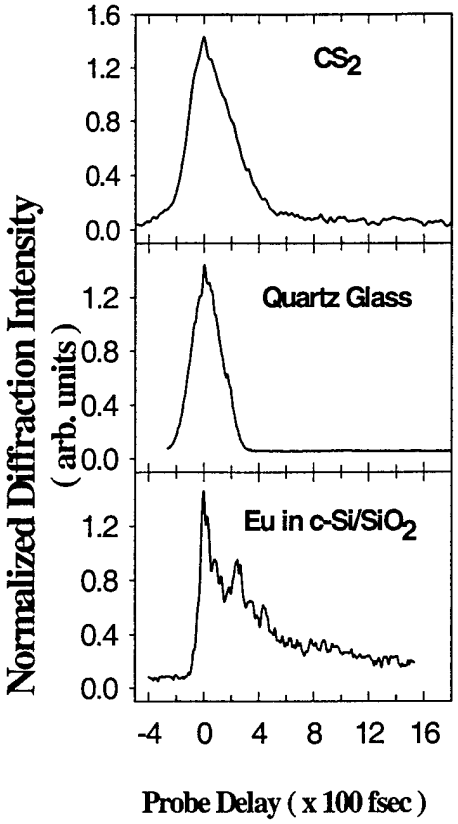

Figure 7. Optical response signal versus probe pulse delay in femtosecond or nanosecond regime. The left part of the figure was obtained using fs-laser system with pulse width of 140fs while the right part was using ps-laser with pulse width of 30ps.

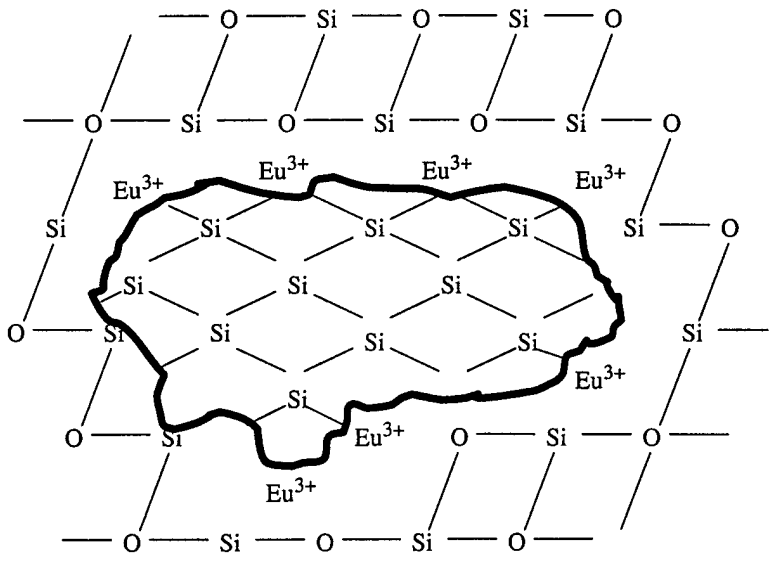

Figure 8. Schematic of Eu-doped nanoparticle c-Si/SiO_2. Eu^{3+} ions are distributed on the boundary surface of c-Si nanoparticles. When the charge carriers produced in CB of the c-Si nanoparticles the carriers can be captured by surrounding Eu^{3+} ions within a short distance due to strong Coulomb interaction

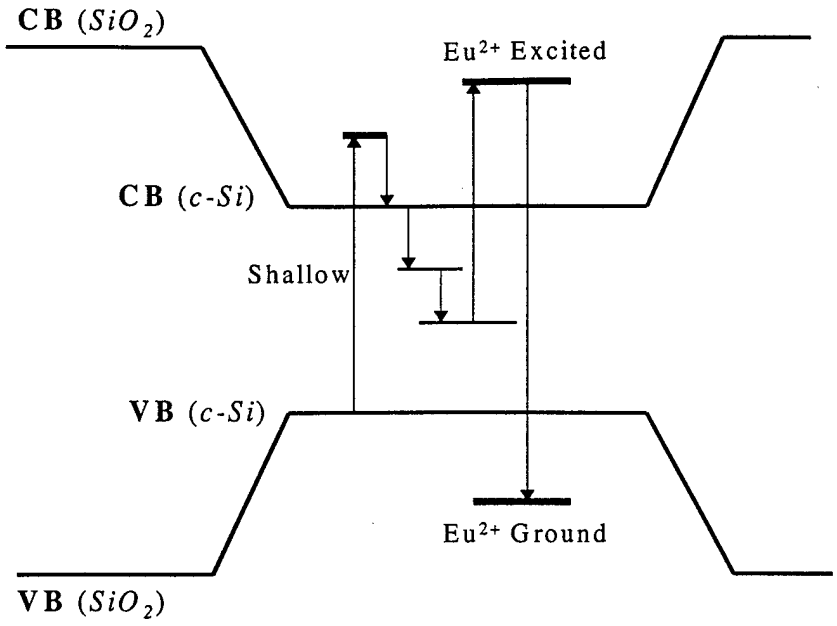

Figure 9. The proposed band structure suggests that upon laser excitation the created charge carriers trapped to form so-called shallow center in nondoping c-Si/SiO_2 material. In Eu-doped sample Eu^{2+} can be formed immediately through charge transfer process. The excitation of Eu^{2+} ions could be realized either through transition from intermediate state within the gap or through TPA from ground state.

The observed slowly decaying signal is recognized as associated with the "excited state grating" which is attributed to the free carriers generated by laser excitation and followed by trapping at the shallow center. It alters the susceptibility of the CB versus VB. In the recombination process the shallow center becomes reactivated. Through a radiative transition the recombination process is completed with a photon emitted. This is in agreement with the PL observation. An additional contribution altering the susceptibility observed in nondoping sample, that is shown as a buildup right after the instantaneous response is presumably associated with the drift motion of the free carriers inside the nanoparticles. Due to the space charge field, originally produced by interference pattern $I = I_0 \exp(-\alpha x/\cos\theta)(1+m\cdot\cos Kz)$, of two crossing laser beams, the carriers move toward one direction within the small nanoparticles

of 1 – 2 nm which is much smaller than the fringe spacing. The formed shallow centers are likely to be on one end or another inside the nanoparticles. The observed buildup period of 400ps is probably related to the collective aggregation of carriers along the grating vector on a macroscopic point of view. In Eu^{3+}-doped c-Si/SiO_2, after laser excitation the created charge carriers undergo a fast movement along all direction toward Eu^{3+} ions which act as point charges reside on the Si/SiO_2 boundary surface. The strong Coulomb interaction results in the shortening of carrier motion period prior to being captured by Eu^{3+}. From the fs-measurement (the bottom of the left part in Fig.7) it is estimated to be a few hundred femtosecons. Note that after capturing a charge Eu^{3+} ion temporarily becomes a divalent Eu^{2+} ion. Eu^{2+} ions possess half-filled 4f shell, and its excited state ^6P has a relatively larger shift of parabolic bottom from the one of the ground state ^6S. This could contribute to alter the susceptibility when excitation transition occurs. The creation of divalent europium ions has been verified by PL measurement as mentioned above. However, either for trivalent or for divalent europium ions the contribution to alter the susceptibility due to excited state population is negligibly small as seen in Eu-doped SiO_2 (the top of the right part in Fig.7). Presumably it is because the amount of Eu^{2+} ions is too small to affect the SR signal. That is why the buildup of the SR signal shown in nondoping sample disappears in Eu-doped sample, and it is also why the emission of Eu^{2+} is so weak.

It should be pointed out that the free-carrier contribution to the change in susceptibility, as seen in laser-induced gratings in most semiconductors [46,47], is also observed here as a slowly decaying, long lasting tail. However, this contribution seems to be not applied to the fast response on the time scale corresponding to the autocorrelation width of the two write-beams. This kind of contribution was observed in poled $KNbO_3$ [48,49], where the signal decay curve had a sharp peak at zero-delay with a long, slow-decay tail. It usually results in a signal buildup in the range of 10 - 100 ps and depending on the crossing angle of the two write-beams. In fact, the observed buildup of the SR response in nondoping sample exhibits no discernible difference except for a relatively longer buildup period. It is believed to be due to the nanoparticle nature that the diffusion process is no longer continuous, and is stopped by 1-2 nm in length.

Based on the above observations a model of structure of Eu-doped nanoparticle c-Si/SiO_2 can

be represented as shown in Fig. 8. Nanoclusters of silicon in the SiO_2 matrix are under the essentially random defect fields with atom-scale size. As a result, the bottom of Si-nanoparticle conduction band (which is assumed approximately corresponded to $k_i \sim 0.85\ k_{max}$, as in the perfect crystal due to multi-valley structure of silicon conduction band) is under the action of strong atomic scale spatial fluctuations. Note that ~20Å size of Si nanoparticle is enough for formation of the bottom of conduction band similar to the perfect Si-matrix. The latter is connected with its minimum at $k_i \sim 0.85\ k_{max}$. Only k-values satisfying $k < (\pi/L)$ inequality, where L is the size of nanoparticle, corresponded to principally different states for the nanoparticle case. The fluctuations induce the spatial multi-well atom-scale structure of conduction band edge. As shown in Fig.9, the latter gives rise to conduction electrons localization in these wells and is accompanied by rather slow hopping diffusion of conduction electrons in such wells system. This model allows explanation of slow diffusion of conduction photoelectrons detected in the experiment for Si-nanoparticles in SiO_2 matrix without Eu impurity doping. When Eu^{3+} impurity ion is located in the interface region of Si-nanoparticle embedded in the SiO_2-matrix, it acts as an attractive Coulomb center for the photoelectron. The center will be the core of the localized electronic state. The energy gap between conduction and valence bands for the Si-nanoparticle is much less than for the SiO_2 matrix. Electrons and holes both are within a deep potential well in the region of nanoparticle. It is important to underline that the shallow state radius of the state induced by of Eu^{3+} Coulomb effect is $r_c \sim 8$ Å within the effective mass approximation, while nanoparticle state corresponding to localization within the above mentioned deep potential well in nanoparticle region, has the state radius $r_{nano} = (L/\pi) \sim$ 7Å. As a result, two large radius shallow states will have the energy splitting at the order of ~ 0.3 eV, much higher than Debye energy. Another important feature is connected with the1s-contribution to the ground state, which corresponds to pronounced electron density on the Eu^{3+} impurity, in which a strong interaction exists between large radius electronic ground state and core electronic state of Eu^{3+}. The excited state $^5D_0$ level of Eu^{3+} in c-Si/SiO_2 thin film is situated below the CB but above the shallow centers of nanoparticle Si. A strong interaction with c-Si

nanoparticles is expected to be the cause of the charge transfer among them. Upon laser excitation at 532 nm (TPA process), the photoinduced carriers produced in CB are trapped at shallow centers and holes in the valence band form an exciton. Because a strong Coulomb' interaction between Eu^{3+} and carriers a transient charge transfer occurs via $(Eu^{3+} + e) = Eu^{2+}$. When low-powered laser excitation is applied the photoluminescence observed is dominated by Eu^{3+} emission. When the increased excitation level applied a new broadband PL attributed to Eu^{2+} through charge transfer was observed. This process was further verified by DFWM experiment, in which the created charge carriers undergo a relatively longer drift motion with an average time period of 400 ps in nondoping sample was found to be shortened in Eu-doped sample.

IV. STUDY OF LUMINESCENT MATERIALS FOR DISPLAY APPLICATIONS

1) Trapping dynamics in $SrAl_2O_4:Eu^{2+},Dy^{3+}$:

We have developed several new phosphorous materials in auspice of the current DoD grant. These include the red phosphor $CaAl_4O_7:Eu^{3+}$, the blue phosphor $SrAl_4O_7:Eu^{2+}$, and persistent green phosphor $SrAl_2O_4:Eu^{2+}$, Dy^{3+}. In the current year, we have spent more time on the study of phosphorescent dynamics, especially on trapping dynamics in persistent phosphors. At first, we have successfully grown single crystal fibers of $SrAl_2O_4$:Eu,Dy. Single crystals are more suitable for study of trapping mechanism.

Trapping centers play an essential role in persistent, photo-stimulable, and thermo-luminescent phosphors, or simply photo-energy storage phosphors. It is the trapping centers that the information of excitation radiations, such as β-ray, γ-ray, x-ray and UV light, can be stored in the phosphors, and then released through thermal or optical activations. If the thermal activation occurs at room temperature, the materials will show an afterglow and are called persistent phosphors. These storage phosphors have been widely used as luminescent paints, dosimetry for high-energy radiation, radiography, and archeology dating. Trapping centers or impurity energy levels in semiconductors have been a topic of long standing which has been studied extensively.

This has not been the case for insulating persistent phosphors; the nature and structure of trapping centers in these materials have not been investigated in any detail due to their complexity of their behavior.

Trapping centers in phosphors can be charge defects or the doping or activator ions themselves. In the persistent green phosphor $SrAl_2O_4:Eu^{2+},Dy^{3+}$, the Dy^{3+} ions are considered to be the source of traps. However, the nature and detailed structure of trapping centers in the material have not been established convincingly and a number of fundamental questions remain. It is obvious that the study and understanding of the nature of each trapping center is the key to the improvement of energy storage efficiency and performance of these materials. Some traps can serve as quenching centers and adversely affect the efficiency of a luminescent material. Questions have been raised as to whether the Dy ion is in a trivalent or in a divalent state and whether it acts as an electron or hole trapping center. For the lanthanide series, the $4f^0(La^{3+})$ and $4f^7(Gd^{3+})$ electronic configurations are relatively stable. Trivalent ions having one or two more 4f electrons beyond these configurations, such as Ce^{3+} ($4f^1$), Pr^{3+} ($4f^2$), Tb^{3+} ($4f^8$) and Dy^{3+} ($4f^9$), can be easily oxidized into the tetravalent state. It follows that Dy ions in solids are prevalently found in a trivalent or tetravalent state rather than in the divalent state. As it is also generally known, intraconfigurational electronic transitions of Dy^{3+} are LaPorte forbidden and are generally weaker than 5d transitions of Eu^{2+}. Sharp line spectra in both samples of $SrAl_2O_4:Eu,Dy$ and $SrAl_2O_4:Dy$ were observed and identified as due to Dy^{3+} and confirms the presence of the trivalent state.

In an electronic trapping model, Dy^{3+} captures an electron from excited Eu^{2+} through the conduction band or directly from the excited ion. This process would transform Dy to its divalent state and Eu to an excited trivalent state $*Eu^{3+}$. If this is the case, the ground state of Dy^{3+} should be near to the bottom of the conduction band or the metastable 4f5d state of Eu^{2+}. Fluorescence and excitation spectra of $SrAl_2O_4:Dy^{3+}$, however, indicate that the ground state of Dy^{3+} is in fact close to the top of the valence band; in addition and as we have argued above, Dy^{2+} is unstable and does not normally exist in solids. This would seem to argue against Dy^{3+} to serving as electronic traps to produce the phosphorescence. A more plausible model proposed is

that Dy^{3+} serves as hole traps. Upon excitation Eu^{2+} may capture one electron from the valence band, becoming an excited monovalent ion, $*Eu^{+}$, and leaving a hole in the band. Dy^{3+} can capture this hole and change valence to Dy^{4+}. Upon thermal activation, Dy^{4+} can release the hole to the valence band reversing the process and producing the afterglow from the excited Eu^{2+} ion.

The hole trapping model is consistent with the observation of afterglow when the sample is pumped at the long wavelength side of absorption band of Eu^{2+}. In addition, the excitation spectra of photoconductivity are also consistent with this model. A photoconductivity peak appeared near the absorption band of Eu^{2+} with energy well below the band gap of $SrAl_2O_4$ (6.6eV). Since no photoelectrons are promoted into the conduction band by the photo-excitation, the photoconductivity peak originates from hole conduction in the valence band.

The fine structures of the thermoluminescence curves for the single crystal can be well resolved and demonstrate the existence of multiple traps. In the aluminate crystal structure, there are two nonequivalent Sr sites or which Dy can substitute. These nonequivalent Dy sites may be responsible for the 280 K and 310K thermal peaks. The broad thermal peak near 400K might be related with the upper stark levels of Dy^{4+}. The thermoluminescence curves do not depend on the population of traps (irradiation time of samples) very much. This implies that retrapping process in this material is negligible and that first order trapping dynamics should apply.

We also applied for first time the photostimilation technique to persistent phosphors. It was surprisingly found that the decay of photostimulated fluorescence is three times faster than the decay of the normal photoluminescence of Eu^{2+} in $SrAl_2O_4:Eu^{2+},Dy^{3+}$. The physical mechanism is unclear. It is tentatively attributed to the fast lattice relaxation of the Eu^{2+} ions, which have been in much distorted lattice environment when their excited electrons were trapped by the trapping center.

2) Trapping centers in $CaS:Eu^{2+},Tm^{3+}$:

As an extension of this study, trapping dynamics of $CaS:Eu^{2+},Tm^{3+}$ was also studied. Alkaline earth sulfides have been intensively studied due to important applications in display

technology. $CaS:Eu^{2+},Tm^{3+}$ is a unique red persistent phosphor and has long been studied. Tm^{3+} is generally thought to be the trapping center. However, our thermoluminescence data reveal that it is the charge defects (Ca vacancies or interstitial S), created by substituting Ca^{2+} with Tm^{3+}, to serve as hole trapping centers, which are responsible for the red afterglow at room temperature. A further investigation of thermoluminescence at higher temperatures indicates that Tm^{3+} serves a deep electronic center. It can capture electrons through the conduction band or directly from excited Eu^{2+} ions. These two processes have different energy barriers, which corresponding to the two observed thermoluminescence peaks at 375K and 545K. When the materials was pumped by the 514.5nm (2.4eV) Ar laser beam, which can not reach a transition from the ground state of Eu^{2+} to the conduction band (the band gap of CaS is 4.2 eV), only 375K thermal peak was observed. The result provides further evidence to support the model proposed.

The above result is of practical significance. It predicts that (1) the afterglow can be greatly reduced by codoping monovalent alkaline ions such as Na^{+} to remove charge defects in $CaS:Eu^{2+},Tm^{3+}$. This has been proved. Reduction of the afterglow was observed in $CaS:Eu^{2+},Tm^{3+},Na^{+}$. The idea can be applied to the case, such as photo storage phosphor $CaS:Eu^{2+},Sm^{3+}$, where afterglow is unwanted; (2) any trivalent ions doped into $CaS:Eu^{3+}$ may create charge defects and to produce afterglow. Strong afterglow was indeed observed in $CaS:Eu^{2+},Al^{3+}$ and $CaS:Eu^{2+},Y^{3+}$; (3) $CaS:Eu^{2+},Tm^{3+}$ can be used as a photostimulable phosphor as in the case of $CaS:Eu^{2+},Sm^{3+}$. To prove this, a further work is under the way.

V. SPECTROSCOPIC STUDY ON SOL-GEL BASED LUMINESCENT MATERIALS

1) Spectroscopy of Cr^{5+}

In addition, study of laser spectroscopy of Cr^{5+} doped in SiO_2 sol-gel glasses has been continued. Since Cr^{2+}, Cr^{3+} and Cr^{4+} are all lasing ions, optical properties of Cr^{5+} should be also interesting. Strong broad band emissions at 620nm and 560nm was observed in Cr^{5+} doped and Cr^{5+} clusters embedded SiO_2 sol-gel glasses, respectively. The intensity of the fluorescence of Cr^{5+} nanoclusters embedded SiO_2 samples degraded slowly with exposure time to laser irradiation. The phenomenon is ascribe to the migration of Cr^{5+} nanoclusters on the surface of

pores due to thermal heating.

2) Study on nanostructured materials Eu^{3+} doped and Eu^{3+}-Y^{3+} codoped SiO_2 sol-gel glasses:

Eu^{3+} doped SiO_2 sol-gel glasses are very interesting materials for luminescence applications, and have been extensively studied in recent years. The red emission of $^5D_0$ to $^5F_2$ near 615 nm and the convenience of thin film preparation through sol-gel technology offer potential advantages for emissive displays. On the other hand, the material has shown persistent high temperature spectral hole burning. Hole burning has been suggested as the physical basis for high density frequency-domain optical data storage. Eu-SiO_2 glasses have shown favorable spectroscopic features for this application: wide inhomogeneous linewidths, high transparency, and high hole persistent temperature (78K). The mechanism of the persistence of the spectral hole observed in the Eu doped Silica glass is unclear. It was generally ascribed to certain photophysical process. Nogami and Hayakawa correlated it with water molecules entrapped in the sol-gel silica glasses. We have conducted a detailed spectroscopic study in the past year in order to understand the physical processes, which govern the spectral hole burning.

3).Effects of annealing on the luminescence:

The samples of Eu^{3+}-doped and Eu^{3+},Y^{3+} co-doped SiO_2 glasses were prepared by the sol-gel method. The dry gels were annealed in air at temperatures from 130 to 1000°C for two hours. Annealing has been widely used to reduce or eliminate residual hydroxyl in sol-gel glasses and to densify the samples. In general, the organic residuals have high vibration frequencies and can efficiently quench luminescence of optically active ions. The intensity of the luminescence was found to obviously increase with annealing temperature due to the reduction of the quenching centers.

The second important effect of annealing is to activate the lattice relaxation of the glass network and ion migration in the glass host. The solubility of rare earths in SiO_2 glass is very limited. During the annealing process, the rare earth ions migrate and form clusters. The clustering process makes the local concentration of Eu very high and causes serious fluorescence

quenching in single doped systems. Consequently, the luminescent intensity is relatively low and the lifetime is shorter. After annealing above 800 °C, the lifetimes of the luminescence of Eu doped samples are still far below the normal value (1.5 to 2.0 ms) of the lifetime of Eu in most crystals. This is ascribed to the concentration quenching. Although the nominal concentration (1at%) in the silica samples prepared in this work is not very high, the real local concentration of Eu can be much higher owing to clustering in the single doped samples.

In addition, the clusterization also changes the symmetry of the lattice environment of Eu^{3+} ions. The transition $^5D_0$ to $^7F_0$ is both spin and electric dipole forbidden and gives rise to a weak peak at 578 nm. The transitions of $^5D_0$ to $^7F_1$ at 587, 592 and 598 nm are magnetic dipole allowed and less sensitive to the lattice environment. It is a dominant transition for Eu ions in an environment with inversion symmetry. On the other hand, the $^5D_0$ to $^7F_2$ transitions at 613, 616, 626 nm are parity (electric dipole) forbidden. It becomes allowed when the lattice environment is distorted and contains non-inversion symmetry. The relative intensities of transitions to $^7F_1$ and $^7F_2$ indicates that Eu ions in the dry gels are present in an environment with near inversion symmetry. With increasing annealing temperature, Eu ions migrate and form clusters of Eu. Eu_2O_3 is monoclinic without inversion symmetry, and the transition $^5D_0$ to $^7F_2$ is dominant. The spectral result indicates that clusterization of Eu is initiated in the annealing process.

4) Effects of Codoping with Y^{3+}

With heavy codoping of Y_2O_3, the luminescent intensity of Eu was found to be greatly increased, and the lifetime became much longer than single doped samples. It is assumed that Eu^{3+} ions prefer to enter into Y_2O_3 nanoclusters which are expected to form in silica matrix. The concentration quenching of luminescence can be therefore greatly reduced due to the dilution of Eu.

In measurements of spectral hole burning, it was found that the critical temperature, at which spectral holes could be burnt, depended on the linewidths of the pump laser beams. With a narrow bandwidth laser, holes could be burnt only up to 35 K. The observed hole widths are

unusually wide for the glasses, about 1 GHz ($0.03cm^{-1}$), more than 30 times broader than that observed in regular Eu doped melt glasses. With increasing temperature, the hole width exhibits a temperature dependence of T^{α} with $1 < \alpha < 1.3$ (Fig. 3), as has been observed in a number of melt glasses. A similar temperature dependence of the homogeneous line width was obtained with fluorescence line narrowing (FLN). However, the hole width is three times wider than the FLN linewidth, suggesting that there exists a fast spectral diffusion process. Much narrower holes in the Eu-Y co-doped glasses ($0.03cm^{-1}$, compared with 0.1 cm^{-1} in 1Eu%:SiO_2 at 5K) is observed. Using a laser with a wider linewidth (0.15 cm^{-1}), a hole with a width of 0.3 cm^{-1} could be burnt at 78 K.

Annealing temperatures significantly affected the spectral hole burning. No persistent holes were observed in the samples un-annealed or annealed below 200 °C or above 1000 °C. The maximum hole depth, 35%, was observed in the sample annealed at 400 °C. The influence might be associated with the physical mechanism producing the spectral holes. Nogami and Hayakawa proposed that the formation of the spectral holes were due to reorientation of water molecules bound with Eu ions, since the hole depth and the water content were both reduced in the samples with annealing temperature and annealing period. However, such correlation between these two events may be just a coincidence. All organic groups were decomposed and released with annealing. Due to the OH vibration quenching, the content of water may not be an important factor for producing a spectral hole. The excitation photo energy stored in the excited ions could be quickly released through nonradiative multiple phonon processes, i.e. vibration quenching. Then the excited Eu ions could immediately return to the initial state and participate in absorption again. In other word, no persistent hole could be observed as seen in the case of un-annealed samples.

The existence of clusterization is an indication that the Eu ions in the sol-gel SiO_2 are not strongly bound with the porous glass network, and relatively mobile. Laser excitation may serve as a driving force to move the excited ions (or their ligands) to a quasi-stable state (potential minimum), and leave a spectral hole there. After clusteriation and densification, Eu ions are

more strongly bound within the clusters and the contribution to the persistent hole becomes smaller.

5) Nanoclusters of Eu^{3+} and Eu^{3+}-Y^{3+}:

Although all the spectroscopic results support the model of clusterization, the microstructure of the clusters is not clear. Y_2O_3 crystals have a cubic structure, while nanoparticles of Y_2O_3 were found to be monoclinic. Bihari et al showed that there were three nonequivalent sites of Eu in the monoclinic nanoparticles. Three groups of emission lines were resolved. The fluorescence lifetimes of the three site Eu ions are different. Inhomogeneous broadening of the luminescence in our samples does not allow us to resolve the fine spectral structure. However, it is very interesting to note that the decay of luminescence of Eu,Y:SiO_2 is almost exponential, in contrast to that of single doped sample Eu:SiO_2, which is nonexponential. This indicates that the clusters related with Y^{3+} may not have the same microstructure as the nanoparticles studied by Bihari et al. It may not be pure clusters of rare earth oxides. It is likely that there exist some kinds of rare earth rich regions, in which the sites of Eu ions are almost equivalent and have a similar decay time.

Raman scattering from undoped, Eu single doped and Eu-Y codoped SiO_2 were measured. A broad band between 400 and 550 cm^{-1} is obviously related with Y-O or Eu-O vibrations. The results indicate that the clusters must be very small and in an amorphous state. TEM micrographs have been taken on the 1%Eu,10%Y doped SiO_2 samples, annealed at 600 and 900 °C. Due to the similar contrast of Si and Y, it is difficult to make clear identification of Y clusters. Some darker dots with a size of subnanometer scale might be related with such clusters.

Conclusion:

Eu doped and Eu,Y codoped silica glasses were prepared by the sol-gel method. Annealing can be used to exclude the entrapped hydroxyl and organic groups in the samples, reduce OH vibration quenching, and consequently increase the luminescence intensity. Due to

the lattice rearrangement during annealing, which eventually leads to clusterization of Eu ions, the local Eu environment changed from one of near inversion to one with relatively more non-inversion symmetry. As a result, the $^5D_0$ red emission to $^7F_2$ becomes more allowed and dominates over the emission lines to $^7F_0$ and $^7F_1$. However, the clusterization caused concentration quenching, shortened the lifetime and limited the improvement of luminescence.

On the other hand, annealing at higher temperatures resulted in denser samples, where the lattice bonding becomes harder and Eu ions tend to form clusters. This might be the reason for the reduction of the spectral hole depth and eventually inhibition of the persistent hole burning for samples annealed at the highest temperatures.

Codoping with Y^{3+}, could inhibit the clusterization of Eu ion since Eu ions may prefer to enter into Y clusters and be therefore diluted. Evidence for this includes the fact that codoping further increased the luminescence intensity and the lifetime of Eu, along with the reduction in the spectral hole width.

VI. DEVELOPMENT OF THEORETICAL MODEL: CHARGE TRANSFER VIBRONIC EXCITONS IN PEROVSKITE-LIKE SYSTEMS

The statement of the problem in the present work based on the important role of the soft TO modes in the formation of absolute diffraction efficiency (ADE) of laser-induced transient gratings in ferroelectric materials like KTa(1-x)Nb(x)O(3) (KTN) solid solution [50]. As it was shown in [50] the main mechanism of optical response appearance can be in this case the effect of charge transfer vibronic excitons (CTVE) [29]. It was predicted on the basis of [51] that the passing of the ferroelectric phase transition (FPT) point leads to the strong peak-like dependence of ADE from concentration (x) or from temperature. The first such tipe experimental study was performed in [52] where the beginning of peak-like ADE x-dependence from both sides of low and high x-values was obtained in the case. In this work we present the results of experimental and theoretical study the influence of FPT in KTN on ADE formation within degenerate four wave mixing method. The well-defined peak-like x-dependences of ADE was detected in KTN

in the region of FPT for slow optical response (SR) as well as for instantaneous response (IR). But if the peak position for SR is near to x = 0.5, the peak position for IR is near to x = 0.33. Some second rather smooth peak with maximum near x = 0.33 in the case of SR can be interpreted. These data can be explained on the basis of CTVE model of optical response [50] with taking into account of the actual two different type of Nb-dipole ordering in KTN. Firstly, this is glass-like ordering in the system of polar nanodomains. The latter is reflected by tending to divergency of nonlinear susceptibility (R.Pirc, B. Tadic, R.Blinc) which leads to strong ADE-peak in nonlinear IR signal (near xg 0.33) and to smooth and rather weak ADE-peak in SR signal in the same region. Secondly, this is ferroelectric type ordering of polar nanodomains which is reflected by tending to divergency of linear susceptibility. The latter leads to strong ADE-peak in SR signal (near FPT point xc 0.5). The method of separation of glass-like and ferroelectric type ordering on the basis of IR and SR signals of ADE study is proposed. Semi-empirical Hartree-Fock calculations of the structure of CTVE and CTVE-phase states in KTaO(3) using the intermediate neglect of differential overlap (INDO) method are performed. The calculations of phonon spectra of CTVE-phase in KTaO(3) made on the basis of dynamical model had allowed to discover new soft modes which are induced by charge transfer. The CTVE phase is formed self-consistently due to interaction between CTVE and these soft modes.

The incipient perovskite-like ferroelectrics with off-center impurities, namely, $KTaO_3$ (KTO) with Li, Nb, Na impurities, $SrTiO_3$ (STO) with Ca impurities are under the high interest at least more than last twenty years [53-54]. This circumstance connects with the appearance of impurity induced ferroelectric phase transition as well as glass-like states controlled by impurity concentration on the one hand, and with the rather complicated and, in spite of model character of these systems, in some aspects unclear physical nature of induced phase transitions on the other. It is especially characteristic for KTO:Nb (KTN) case where we have to deal with a weak off-center effect for single impurity ion. The phenomenon model based on the self-ordered impurity clusters which obey the order-disorder type as well as the low-frequency displacive type degrees of freedom of such clusters was proposed. But verification of this model and the solving of problem of impurity induced ferroelectric phase transition need new experimental

information about these phase transitions in the ferroelectric oxygen-octahedral perovskites under consideration.

The latter effect might be important in the region of impurity induced ferroelectric phase transition. In particular, the central peak phenomenon induced by light can change the soft mode critical dependence.

1) Carge transfer vibronic excitons in ferroelectric oxides: experiment and theory

The development of charge transfer vibronic excitons (CTVE) study in ferroelectric oxides has been reviewed. CTVE is the correlated pair of electronic and hole small polarons which stability is controlled by pair

pseudo-Jahn-Teller effect with pronounced "Negative-U" effect [56-58]. Corresponded potential well becomes more deep in soft matrices like ferroelectric oxides. The consideration is focused on the phenomena induced by CTVE. Namely, there are (i) mechanisms of optical response and absolute diffraction efficiency formation of the laser-induced transient gratings in KTa(1-x)Nb(x)O(3) [50], and the mechanisms of energy migration [50] in this situation; (ii) drastic shift of the edge of fundamental absorption with temperature in SBN [59], (iii) polar microdomains in incipient ferroelectrics KTaO(3) and SrTiO(3) as well as in KTaO(3):Li [60,61], and the appearance of low temperature uncommon state (Müller phase) in SrTiO(3) [57,58]. Semi-empirical Hartree-Fock calculations of structure of CTVE, of their extended clusters, and of CTVE-phase [58,59] (where CTVE exist in each cell) are performed. The calculation of phonon spectra of CTVE-phase [62] had allowed to discover the soft modes induced by charge transfer. Their condensation leads to CTVE energy lowering which determines the equilibrium values of charge transfer in excitons under consideration. Here the set of CTVE is appeared. It is also shown that the role of one charged oxygen vacancies is not only in admixture of CTVE phase states, but also in the increasing of dipole-dipole correlations and of corresponding order parameter in CTVE phase. The latter is due to tunneling of trapped electron on the vacancy in the new charge transfer state. We consider also the reorienting degrees of freedom of CTVE, and CTVE clusters (for instance, CTVE clusters induced by defect

fields due to admixture of CTVE phase states) as tunneling pseudospins which can be taken into account on the basis of Ising model with transversal field. This circumstance can be, probably, the origin of the success of the use of Ising model with transversal field in the study of ferroelectric oxides.

2) Critical effects in optical response due to charge transfer vibronic excitons and their structure in perovskite-like systems

The statement of the problem in our work based on the important role of the soft TO modes in the formation of absolute diffraction efficiency (ADE) of laser-induced transient gratings in ferroelectric materials like KTa(1-x)Nb(x)O(3) (KTN) solid solution [50]. As it was shown in [28] the main mechanism of optical response appearance can be in this case the effect of charge transfer vibronic excitons (CTVE) [56]. It was predicted on the basis of [50] that the passing of the ferroelectric phase transition (FPT) point leads to the strong peak-like dependence of ADE from concentration (x) or from temperature. The first such tipe experimental study was performed in [52] where the beginning of peak-like ADE x-dependence from both sides of low and high x-values was obtained in the case. In this work we present the results of experimental and theoretical study the influence of FPT in KTN on ADE formation within degenerate four wave mixing method. The well-defined peak-like x-dependences of ADE was detected in KTN in the region of FPT for slow optical response (SR) as well as for instantaneous response (IR). But if the peak position for SR is near to x = 0.5, the peak position for IR is near to x = 0.33. Some second rather smooth peak with maximum near x = 0.33 in the case of SR can be interpreted. These data can be explained on the basis of CTVE model of optical response [50] with taking into account of the actual two different type of Nb-dipole ordering in KTN.

Firstly, this is glass-like ordering in the system of polar nanodomains. The latter is reflected by tending to divergency of nonlinear susceptibility (R.Pirc, B. Tadic, R.Blinc) which leads to strong ADE-peak in nonlinear IR signal (near xg = 0.33) and to smooth and rather weak ADE-peak in SR signal in the same region. Secondly, this is ferroelectric type ordering of polar nanodomains which is reflected by tending to divergency of linear susceptibility. The latter leads

to strong ADE-peak in SR signal (near FPT point xc = 0.5). The method of separation of glass-like and ferroelectric type ordering on the basis of IR and SR signals of ADE study is proposed. Semi-empirical Hartree-Fock calculations of the structure of CTVE and CTVE-phase states in KTaO(3) using the intermediate neglect of differential overlap (INDO) method are performed. The calculations of phonon spectra of CTVE-phase in KTaO(3) made on the basis of dynamical model had allowed to discover new soft modes which are induced by charge transfer. The CTVE phase is formed self-consistently due to interaction between CTVE and these soft modes.

4. LISTING OF ALL PUBLICATIONS AND TECHNICAL REPORTS

SUPPORTED UNDER THIS GRANT

(a) Papers published in peer-reviewed journals:

1) H.Liu, Y.Wang, W.Jia and F.Fernandez, "Excitation dynamics of cerium in niobate crystals". **Jour. Alloys & Comp., 250 (1997)360.**

2) H.Liu, Y.Wang, W.Jia, "Formation of small poraron by two-photon excitation in niobate crystals" **J.Lumin., 72-74 (1997)945.**

3) J.D.Romero, H.Liu and W.Jia, "dispersion effects of population grating in Cr-doped YAG crystal by four wavemixing" **J.Lumin., 72-74 (1997)854.**

4) H.Liu and W.Jia, "Validity using pump-probe pulses to determine the optical response of niobate crystals", **NASA URC-TC,** ed. M.Jamshidi et al., Vol.**1, pg.465, 1997**, Albuqueque.

5) J.Zhang, H.Liu, W.Jia, "Investigation into self-pumped and mutually-pumped phase conjugation with beams entering the negative C-face of doped $(K_{0.5}Na_{0.5})_{0.2}(Sr_{0.75}Ba_{0.25})_{0.9}Nb_2O_6$ crystals", **Applied Optics, 36 (1997) 3753.**

6) J.Yu, H.Liu, Y.Wang, F.E.Fernandez, W.Jia,"Irradiation induced luminescence enhancement effect of ZnS:Mn^{2+} nanoparticles in polymer films", **Opt.Lett., 22 (1997) 913.**

7) H.Liu, W.Jia,"Photoluminescence and fast nonlinear optical response of barium titanate crystals", **J.Lumin., 76/77 (1998)100.**

8) J.Yu, H.Liu, Y.Wang, F.E.Fernandez, W.Jia,"Optical properties of ZnS:Mn^{2+} nanoparticles in polymer films", **J.Lumin., 76/77 (1998) 252.**

9) W.Jia, H.Yuan, L.Lu, H.Liu, W.M.Yen, "Phosphorescent Dynamics in $SrAl_2O_4$:Eu^{2+}, Dy^{3+} Single Crystal Fibers", **J.Lumin., 76/77 (1998) 424.**

10) L.Castro, W.Jia, Y.Wang, M. Santiago and H.Liu, "Luminescence of Eu^{3+} doped SiO_2 thin films and glass prepared by sol-gel technology" NASA URC-TC, ed. T.L. Coleman et al., **Vol.3, Pg.634, 1998**, TSI Press,Huntsville, AL.

11) W.Jia, L.Castero, Y.Wang and H.Liu, "Fluorescence of pantavalent chromium in SiO_2 Sol-Gel glasses", NASA URC-TC, ed.T.L. Coleman et al., **Vol.3, Pg.639, 1998**, TSI Press,Huntsville, AL.

12) H.Liu, Y.Wang, M. Santiago and W.Jia, "Anisotropically coherent optical-response of Eu-doped yttrium orthosilicate" NASA URC-TC, ed.T.L. Coleman et al., **Vol.3, Pg.848, 1998**, TSI Press, Huntsville, AL.

13) J.Yu, H.Liu, Y.Wang,W.Jia, L.F. Fonseca, S.Z. Weisz and O Resto, "A new analysis method to characterize the S-band luminescence decay of porous Si", **J.Lumin., 81 (1999) 1.**

14) J.Yu, H.Liu, Y.Wang, W.Jia,"Hot luminescence of Mn^{2+} in ZnS nanocrystals", **J.Lumin.,79 (1998) 191.**

15) V. Vikhnin, H.Liu, W.Jia,"Mechanism of energy migration due to charge transfer vibronic excitons: role of ferroelectric phase transition in solid solutions $KTa_{1-x}Nb_xO_3$",**Phys.Letters A 245 (1998) 307**

16) W.Jia, H.Yuan, L.Lu, H.Liu, W.M.Yen, "Crystal growth and characterization of Eu^{2+}, Dy^{3+}:$SrAl_2O_4$ and Eu^{2+}, Nd^{3+}:$CaAl_2O_4$ by the LHPG method", **J.Crys.Growth, 200 (1999)179.**

17) Weiyi Jia, Huimin Liu, Huabiao Yuan, Lizhu Lu and W.M. Yen, "Luminescence Spectra of Divalent Europium Ions Doped in $SrAl_4O_7$", Luminescence Materials IV,**Electrochem. Soc. Proc., 97-29 (1998) 368.**

18) K.S. Hong, R.S. Meltzer, P.Feofilov, A.A. Kaplyanskii, R.I. Zakharchenya, W. Jia, H. Liu, B. Tissue, "Comparison of dynamics of Eu^{3+}in different Y_2O_3 nanostructured materials and sol-gel produced SiO_2 glass" **K J. Lumin., 83-84 (1999) 393.**

19) H. Liu, S.T. Li*, G.K. Liu*, W. Jia and F.E. Fernández, "Optical properties of undoped and Eu^{3+}-doped SBN thin film grown by pulsed laser deposition" **J. Lumin., 83-84 (1999) 367.**

20) V. Vikhnin, H. Liu and W. Jia, "A new model of transient optical response:effect of charge

transfer vibronic excitons", **Phys.Letters A** in press
21) W. Jia, H. Yuan, S.Holmstrom, H. Liu, W. Yen, "Photo-stimulated luminescence in $SrAl_2O_4$: Eu^{2+}, Dy^{3+}single crystal fibers". **J. Lumin., 83-84 (1999) 465.**
22) Huimin Liu, L. F. Fonseca, S. Z. Weisz , W. Jia and O. Resto, "Observation of picosecond nonlinear optical response from porous silicon". **J. Lumin., 83-84 (1999) 37.**
23) H. Liu, S.T. Li, F.E. Fernandez and G.K. Liu, "Characterization of strontium barium niobate optical thin film grown by pulsed laser deposition", "CP497, **Nondestructive Characterization of Materials IX"**, pp.332-338, 1999, Ed. by R.E. Green, Jr., AIP Press.
24) H. Liu, L.F. Fonseca, S. Z. Weisz, Q. Yan, W. Jia and O.Resto "Optical property and picosecond response of porous silicon wafer", "CP497, **Nondestructive Characterization of Materials IX"**, pp.339-345, 1999, Ed. by R.E. Green, Jr.,AIP Press.
25) V. Vikhnin, H.Liu, W.Jia and S. Kapphan,"Charge transfer vibronic excitons in ferroelectric oxides: experiment and theory" **J. Lumin., 83-84 (1999) 91.**
26) V. Vikhnin, H.Liu, W.Jia,S. Kapphan, R. Eglitis and D. Usvayt, "Critical effects in optical response due to charge transfer vibronic excitons and their structure in perovskite-like systems"**J. Lumin., 83-84 (1999) 109.**
27)V. Vikhnin, H.Liu, W.Jia, "Possible Role of Charge Transfer Vibronic Excitons in Light Induced Change of Polarizability in Ferroelectric Solid Solutions Kta1-XNbXO3 ", **Ferroelectrics, 235 (1999) 181.**
28) S.P. Feofilov, K.S. Hong, R.S. Meltzer, W. Jia and H. Liu, "Persistent Spectral Hole-Burning and Fluorescence Line Narrowing Studies of the Homogeneous Linewidth of Eu^{3+} in Sol-Gel Produced SiO_2 Glass", **Phys. Rev.B, 60 (1999) 9406.**
29) Weiyi Jia, Huimin Liu, Sergey P. Feofilov, Richard Meltzer, and Jun Jiao, "Spectrocopic study of Eu^{3+} doped and Eu^{3+},Y^{3+} codoped SiO_2 sol-gel glasses", **J.Alloys and Compouds, 311 (2000) 11.**
30) V.S. Vikhnin, S. Kapphan, H. Liu, W. Jia, V. Trepakov and L. Jastrabik,"Polaron and charge transfer vibronic exciton phenomena in ferroelectrics", **Ferroelectrics, 237 (2000) 81.**
31) F.E. Fernandez, H. Liu C. Jin and W. Jia, "SBN thin film growth by pulsed laser deposition and study of nonlinear optical properties", **Integrated Ferroelectrics, 29 (2000) 111.**
32) S.T. Li and G.K. Liu, H. Liu and F. E. Fernandez, "Effects of thermal annealing on spectroscopic properties of Eu3+ in Sr1-xBxNb2O6 films", **J. Alloys and Compounds, 303-304 (2000)360.**
33) Huimin Liu, Azizz Mafould, Armando Yance, "Aacoustic wave determination by degenerate four-wave-mixing using ultrafast laser pulses" **SPIE Proc., 4072 (2000) 535.**
34) D. Jia, W. Jia, D. R. Evans, W. M. Dennis, H. Liu, J. Zhu, and W. M. Yen, "Trapping processes in CaS:Eu2+ ,Tm3+", **J. Appl Phys. 88 (2000) 3402.**
35) Weiyi Jia, Dongdong Jia, Huabiao Yuan, D.R. Evans, W.M. Dennis, Huimin Liu, Jin Zhu and W.M. Yen, Trapping Centers in Persistent and Thermoluminescent Phosphors, in Physics and Chemistry of Luminescence Materials, eds. By C.R. Ronda, L.E. Shea and A.M. Srivastava, Electrochemical Society Inc., PV99-40 (2000) 211.
36) W. Jia, Y. Wang, J. R.. Jimenez and H. Liu, "Spectroscopy of Cr^{5+} doped and Cr^{5+} Nanoclusters embedded Porous Sol-Gel SiO_2 Glasses", **Colloids and Surface A, 179(2001)185.**
37) W. Jia, D. Jia, H. Yuan, D. R. Evans, W. M. Dennis, H. Liu, J. Zhu, and W. M. Yen, "Trapping centers in persistent and thermoluminescent phosphors", **lectrochem Soc.., 99-40 (2000) pp211-218.**
38) S.T. Li, G.K. Liu, H. Liu and F.E. Fernandez, "Laser spectroscopic studies of crystallization in Eu^{3+}doped $Sr_xBa_{1-x}Nb_2O_6$ films". 22nd Rare Earth Research Conf. July 10-15, 1999, to be published in **Jour.Alloy & Compound**
39) V.S. Vikhnina, H. Liub, W. Jiab, and S.E. Kapphanc "Optics of new polaronic-type excitons in ferroelectric oxides", J.Lumin, accpted for publication.
40) V. S. Vikhnina, S. Avanesyanb, H. Liub, and S. E. Kapphanc, "Visible range in ferroelectric oxides: possible role of charge transfer vibronic excitons" J.Lumin, accpted for publications.

(b) Papers published in nonpeer-reviewed journals or in conference proceedings:

1) H.Liu, Y.Wang, W.Jia, M.Shen and S.Fu, "Nonlinear optical response of polyphenylquinoxaline solution", **Proc.Intern.Conf.Organ.Nonl.Opt.93,** Marco Island, FL, Dec.16-20, 1996.
2) W.Jia and H.Liu, "Up-conversion dynamics of Er^{3+} doped $LiNbO_3$ crystal fibers", **Proc.190th Meeting of the Electrochemical Society,** Oct. 6-10, 1996, San Antonio
3) H.Liu and W.Jia, "Validity using pump-probe pulses to determine the optical response of niobate crystals", NASA URC-TC'97, Feb.16-19, 1997, Albuqueque, NM.
4) H.Liu, W.Jia,"Orientation dependence of fast optical response in barium titanate crystals", Intern.Conf.DPC'97, July 20-24, 1997.
5) W.Jia, H.Liu, H.Yuan, L.Lu and W.M.Yen, "Luminescence spectrum of divalent europium ions doped in $SrAl_4O_7$", **Luminescence Materials IV, Electrochem.Soc.Proc., Vol 97-29 (1998) 368.**
6) H.Yuan, W.M. Dennis, L.Lu, W.M.Yen, W.Jia,and H.Liu, "Photoluminescence of trivalent europium ions doped in $CaAl_4O_7$", **Luminescence Materials IV, Electrochem. Soc. Proc., Vol 97-29 (1998) 206.**
7) W.Jia, H.Yuan, L.Lu, H.Liu and W.M.Yen, "Phosphorescent dynamics of Eu^{2+}, Dy^{3+} codoped $SrAl_2O_4$ single crystal fibers", 6th Intern.Conf.Lumin.Mater., Aug.31-Sept.5, 1997, Paris, France. in press.
8) J.Yu, H.Liu, Y.Wang, F.E.Fernandez, W.Jia,"Optical properties of ZnS:Mn^{2+} nanoparticles in polymer films", Inter.Conf.DPC'97, July 20-24, 1997.
9) W.Jia, H.Yuan, L.Lu, H.Liu, W.M.Yen, "Phosphorescent Dynamics in $SrAl_2O_4$:Eu^{2+}, Dy^{3+} Single Crystal Fibers", Inter.Conf.DPC'97, July 20-24, 1997.
10) W.Jia, H.Yuan, L.Lu, H.Liu and W.M.Yen, "Luminescent spectrum of divalent europium ions doped in strontium di-aluminate", 6th Intern.Conf.Lumin. Mater., Aug.31-Sept.5, 1997, Paris, France.
11) H.Yuan, W.Jia, L.Lu, H.Liu and W.M.Yen, "Photoluminescence of trivalent europium ions doped in calcium di-aluminate", 6th Intern.Conf.Lumin.Mater., Aug.31-Sept.5, 1997, Paris, France.
12) W.Jia, H.Yuan, L.Lu, H.Liu and W.M.Yen, "Phosphorescent dynamics of Eu^{2+},Dy^{3+} codoped $SrAl_2O_4$ single crystal fibers", 6th Intern.Conf.Lumin.Mater., Aug.31-Sept.5, 1997, Paris, France.
13) H.Liu, F. Fernandez, W.Jia, L.A.Boatner, "Transient grating in a $KNbO_3$/$KTaO_3$ superlattice", SPIE Proc.,**Vol. 3425 (1998)182.**
14) H. Liu*, W. Jia, Y. Wang, Y. Fu and L.A. Boatner, "Modulation of the nonlinear optical response by $KNbO_3$ thin films deposited on a $KTaO_3$ substrate", **SPIE Proc. Vol. 3491, (1998)745.**
15) H. Liu*, W. Jia, Y. Wang, Y. Fu and L.A. Boatner, "Modulation of the nonlinear optical response by $KNbO_3$ thin films deposited on a $KTaO_3$ substrate", **SPIE Proc. Vol. 3491, (1998)745.**
16) F.Fernandez, H. Liu, C. Jing, Y.Fu and W. Jia, "SBN thin film growth by pulsed laser deposition and characterization of nonlinear optical properties" Materials Research Society Spring Meeting, Apr.1998,
17) W. Jia, Y. Wang and H. Liu,"Photoluminescence of Eu^{3+} in SiO_2 Sol-Gel glasses" Materials Research Society Spring Meeting, Apr.1998,
18) H.Liu, W.Jia, L.A.Boatner, "Transient grating in a $KNbO_3$/$KTaO_3$ superlattice", SPIE, San Diego, July 19-24,1998.
19) H. Liu*, W. Jia, Y. Wang, Y. Fu, F.Fernandez, L.A. Boatner, "Modulation of the nonlinear optical response by $KNbO_3$ thin films deposited on a $KTaO_3$ substrate", Inter.Conf.Appl.Photon. Ottawa Canada, July 27-30, 1998
20) W. Jia, H. Liu, W. Yen, "Trapping Dynamics in Persistent Phosphors", 196th Meeting of The Electrochemical Society, Inc. Honolulu, Hawaii, October 17-22, 1999, Hilton Hawaiian Village
21) K.S. Hong, R.S. Meltzer, P.Feofilov, A.A. Kaplyanskii, R.I. Zakharchenya, W. Jia, H. Liu, B. Tissue, "Comparison of dynamics of Eu^{3+}in different Y_2O_3 nanostructured materials and sol-gel produced SiO_2 glass" 12th International Conference on Dynamical Processes in excited States of Solids (DPC'99),Puerto Rico, May 23-27, 1999.
22) W. Jia, H. Yuan, S. Holsman, H. Liu, W. Yen, "Photo-stimulated phosphorescence of long

persistent phosphors $SrAl_2O_4$: Eu^{2+}, Dy^{3+}" 12th International Conference on Dynamical Processes in excited States of Solids (DPC'99),Puerto Rico, May 23-27, 1999.
23) Huimin Liu, L. F. Fonseca, S. Z. Weisz , W. Jia and O. Resto, "Observation of picosecond nonlinear optical response from porous silicon" 12th International Conference on Dynamical Processes in excited States of Solids (DPC'99),Puerto Rico, May 23-27, 1999.
24) H. Liu, S.T. Li, G.K. Liu, W. Jia and F.E. Fernández, "Optical properties of undoped and Eu^{3+}-doped SBN thin film
grown by pulsed laser deposition" 12th International Conference on Dynamical Processes in excited States of Solids (DPC'99),Puerto Rico, May 23-27, 1999.
25) H. Liu, S.T. Li, F.E. Fernandez and G.K. Liu, "Characterization of strontium barium niobate optical thin film grown by pulsed laser deposition" Ninth international symposium on nondestructive characterization of Materials Sydney, Australia, June 28-July 2, 1999
26) H. Liu, L.F. Fonseca, S. Z. Weisz, W. Jia and O.Resto "Optical property and picosecond response of porous silicon wafer"Ninth international symposium on nondestructive characterization of Materials Sydney, Australia, June 28-July 2, 1999
27) V. Vikhnin, H.Liu, W.Jia and S. Kapphan,"Charge transfer vibronic excitons in ferroelectric oxides: experiment and theory"Invited Talk, 12th International Conference on Dynamical Processes in excited States of Solids (DPC'99),Puerto Rico, May 23-27, 1999.
28) V. Vikhnin, H.Liu, W.Jia,S. Kapphan, R. Eglitis and D. Usvayt, "Critical effects in optical response due to charge transfer vibronic excitons and their structure in perovskite-like systems" 12th International Conference on Dynamical Processes in excited States of Solids (DPC'99),Puerto Rico, May 23-27, 1999.
29) L.F. Fonseca, S.Z. Weisz, O. Resto, R.K. Soni, H. Liu, W. Jia, M. Gomez, "Comparative analysis of the 1.54 μm emission of Er-doped Si/SiO_2 films and size distribution of the nanostructure" Fifth IUMRS International Conference on Advanced Materials (IUMRS-ICAM'99), Beijing, China, June 13-18, 1999
30) V.S. Vikhnin, S. Kapphan, H. Liu, W. Jia, V. Trepakov and L. Jastrabik,"Polaron and charge transfer vibronic exciton phenomena in ferroelectrics", European Meeting on Ferroelectricity, Pragua, July 1999.
31) S.T. Li, G.K. Liu, H. Liu and F.E. Fernandez, "Laser spectroscopic studies of aser spectroscopic studies of crystallization in Eu^{3+}doped $Sr_xBa_{1-x}Nb_2O_6$ films". 22nd Rare Earth Research Conf. July 10-15, 1999, Argonne National Lab.
32) V.S. Vikhnin* , H. Liu and W. Jia, "Optical response due to charge transfer vibronic excitons: the method of separation of ferroelectric soft mode and glass-like behavior in ferroelectric solid solutions", Ferroelectrics workshop FWPR'99, Guánica, Puerto Rico, May 13-14, 1999.
33) F.E. Fernandez, H. Liu C. Jin and W. Jia, "SBN thin film growth by pulsed laser deposition and characterization of nonlinear optical properties",Ferroelectrics workshop FWPR'99, Guánica, Puerto Rico, May 13-14, 1999.
34) G.A. Nery, A. Mahfoud L.F. Fonseca, H. Liu, O. Resto and S.Z. Weisz, "Study of the luminescence of Eu-doped nanocrystalline Si/SiO_2 systems prepared by RF co-sputtering", Fall MRS meeting, Nov.28 - Dec.3, 1999, Boston, MA.
35)W. Jia, D. Jia, D.R. Evans, W.M. Dennis, H. Liu, J. Zhu and W.M. Yen, "Trapping Centers in Persistent and Thermoluminescent Phosphors", to be published in Proceedings of the Eighth International Symposium on the Physics and Chemistry of Luminescent Materials, Oct.17-22, Honolulu, HI, 1999, ECS Proc. Volumes. (ECS, Pennington, NJ).
36) Huimin Liu, Aziz Mahfoud, G.A. Nery, Luis F. Fonseca, O. Resto and Zvi S. Weisz, "Photoluminescence of Eu^{3+}in Si/SiO_2 nanostructure films" Proc. MRS, Vol.609, Spring meeting, San Francisco, CA, Apr.24-28, 2000. In press.
37) F. Fernandez, Y. Gonzalez, H. Liu, E. Rodriguez, V. Rodriguez, W. Jia, "Pulsed laser deposition growth of SBN and correlation study of structure and optical properties" SPIE Proc.(2000), San Jose, Jan.22-28, 2000. To be published.
38) A. Mahfoud, H. Liu, F.E. Fernandez, "Laser-induced photoluminescence of Eu^{3+} in strontium-barium niobate thin films", NASA URC-TC, Nashville, TN, Apr.10, 2000.
39) V.S. Vikhnin* , H. Liu and W. Jia, "Charge transfer vibronic excitons in laser-induced charges

in polarizability of ferroelectric solid solutions$KTa_{1-x}Nb_xO_3$: the origin of instantaneous and slow optical response" Proc.Inter.Symp. Ferroelectric Relaxor Phys., Dubna, June, 2000, acceptedfor publication.

40) V.S. Vikhnin* , H. Liu and W. Jia, "Charge transfer vibronic excitons in laser-induced charges in polarizability of ferroelectric solid solutions$KTa_{1-x}Nb_xO_3$: the origin of instantaneous and slow optical response" Proc. Inter.Symp.ferroelectrics, Voronezh, Sept. 2000, accepted for publication.

41) V.S. Vikhnin* , H. Liu and W. Jia, "Charge transfer vibronic excitons in laser-induced charges in polarizability of ferroelectric solid solutions$KTa_{1-x}Nb_xO_3$: the origin of instantaneous and slow optical response" Proc.Inter.Conf.Dielectrics -2000, St.Petersburg, Sept.,2000.accepted for publication

42) Iris Rivera, Weiyi Jia, Yanyun Wang, Karem Monge, Huimin Liu and Felix Fernandez,"**Luminescence Spectra and Sensitization of $CaTiO_3:Pr^{3+}$**, NASA URC-TC, Nashville, TN, Apr.10, 2000.

43) Karem Monge, Weiyi Jia, Yanyun Wang, Iris Rivera, Huimin Liu and Felix Fernandez, **Photoluminescence of Pure and Eu^{3+} doped Zno**, NASA URC-TC, Nashville, TN, Apr.10, 2000.

44) W. Jia, D. Jia, H. Yuan, D.R. Evans, W.M. Dennis, H. Liu, J. Zhu and W.M. Yen, "Trapping center in persistent and thermoluminescent phosphors", "Physics and Chemistry of Luminescence materials" edit. By C.R. Ronda, L.E. Shea and A.M. Srivastava, Vol. 99-40, pp.211-218., ISBN 1-56677-263-x, The Electrochemical Society, Pennington, NJ, 2000.

45) G.A. Nery, A. Mahfoud L.F. Fonseca, H. Liu, O. Resto and S.Z. Weisz, "Study of the luminescence of Eu-doped nanocrystalline Si/SiO_2 systems prepared by RF co-sputtering", Mat. Res. Soc. Proc.581, (2000) 647.

46) V.S. Vikhnin, S. Kapphan, H. Liu, W. Jia, V. Trepakov and L. Jastrabik,"Polaron and charge transfer vibronic exciton phenomena in ferroelectrics", **9th European Meeting on Ferroelectrics , July 12-16, 1999**, Praha, Czech.

47) F. Fernandez, Y. Gonzalez, H. Liu, E. Rodriguez, V. Rodriguez, W. Jia, "Pulsed laser deposition growth of SBN and correlation study of structure and optical properties" SPIE 2000, San Jose, Jan.22-28, 2000.

48)Huimin Liu, Aziz Mahfoud, Luis F. Fonseca, Zvi S. Weisz, "Photoluminescence of Eu^{3+}in Si/SiO_2 nanostructure films" submitted for 2000 MRS Spring meeting, San Francisco, CA, Apr.24-28, 2000.

49) Huimin Liu, Azizz Mafould, Armando Yance, "Aacoustic wave determination by degenerate four-wave-mixing using ultrafast laser pulses" 4th Intern.Conf.Vibration Measurements by laser techniques, June 20-23, 2000, Ancona, Italy.

50) G.A. Nery, L.F. Fonseca, H. Liu, O. Resto and S.Z. Weisz, "Effects of the substrate temperature, annealing temperature, and hydrogen presence during sputtering on the luminescence of Eu-doped nanocrystalline Si/SiO_2", MRS Fall Meeting, Boston, Nov.27 - Dec.1, 2000.

51) G.A. Nery, L.F. Fonseca, H. Liu, O. Resto and S.Z. Weisz, "Effects of the substrate temperature, annealing temperature, and hydrogen presence during sputtering on the luminescence of Eu-doped nanocrystalline Si/SiO_2", Proc. MRS, Fall Meeting, Boston, Nov.27 - Dec.1, 2000.

52) H. Liu, A. Mahfoud, V. Vikhnin, S. Avanesean, W. Jia, G. A. Nery, O. Resto, Luis F. Fonseca, Zvi S. Weisz, "Photoinduced charge generation and ultrafast response in Si nanoparticle thin films" The Electr.Chem.Soc,Intern.Semicond.Tech.Conf., May 27, 2001, accepted.

53) H. Liu, S.T. Li, F.E. Fernandez and G.K. Liu," Optical property of Eu in strontium barium niobate optical thin film grown by pulsed laser deposition", Intern.Conf. Rare-earth,2001, accepted.

54) H. Liu, A. Mahfoud, G. A. Nery, O. Resto, Luis F. Fonseca, Zvi S. Weisz, "Ultrafast nonlinear optical property and Eu^{3+} - Eu^{2+} switching in Si/SiO_2 nanocomposites", Intern.Conf. Rare-earth,2001, accepted.

55) H. Liu, A. Mahfoud, V. Vikhnin, S. Avanesean, W. Jia, G. A. Nery, O. Resto, Luis F. Fonseca, Zvi S. Weisz, "Photoinduced charge generation and ultrafast response in Si nanoparticle thin films" The Electr.Chem.Soc,Intern.Semicond.Tech.Conf., May 27, 2001, accepted.

56) H. Liu, S.T. Li, F.E. Fernandez and G.K. Liu," Optical property of Eu in strontium barium niobate optical thin film grown by pulsed laser deposition", Intern.Conf. Rare-earth,2001, accepted.

57) H. Liu, A. Mahfoud, G. A. Nery, O. Resto, Luis F. Fonseca, Zvi S. Weisz, "Ultrafast nonlinear optical property and Eu^{3+} - Eu^{2+} switching in Si/SiO_2 nanocomposites", Intern.Conf. Rare-earth,2001, accepted.
58) Wuliang Xu, Weiyi Jia, Iris Revira, Karem Monge and Huimin Liu, **Optical Properties of Multiple Sites of Eu^{3+} in SrY_2O_4 Single Crystal Fibers**, submitted to J. Electrochem. Soc.

(c) Papers presented at meetings, but not published in conference proceedings:

None

(d) Manuscript submitted, but not published:

1) J.Yu, H.Liu and W.Jia, "Direct manifestation of the configurational coordinate model in hot luminescence of Mn^{2+} in ZnS nanocrystals", submitted to Phys.Rev.Lett., not published.

(e) Technical reports submitted to aro:

1. Annual Progress and Final Progress report:
1) Interim Progress report for 1997.
2) Interim Progress report for 1998.
3) Interim Progress report for 1999.
4) Interim Progress report for 2000.
5) Final Progress report for 1996 -2001. This one.

2. Manuscript and reprint report:
Manuscript report were sent at the time submitted. All reprint reports were sent when reprints received.

5. LIST OF ALL PARTICIPATING SCIENTIFIC PERSONNEL

1) PI. Dr. Huimin Liu, Professor of Physics:
Starting on June 21, 1996 when the notifying letter for funding approval from ARO was received, we immediately work on the project. It was Dr.Liu's responsibility to organize and coordinate the entire project. Dr. Liu devoted most of his time to the research all year around during the project period. He used to work 7 days a week and 11 hours per day. He was working mainly on ultrafast laser spectroscopy and NLO of materials. In the mean time, he supervised postdoctorals, visiting scientists and technicians, as well as graduate students and undergraduate students. During the period he received 1) "Scholarly Productivity Award, The recognition of the most productive researchers in the EPSCoR project for 95-96, 97, 98-99, 00-01; and "Scholarly Productivity Award, The recognition of the most productive researchers in UPR-Mayaguez.

2) Co-PI. Dr. Weiyi Jia, Professor of Physics:
Dr. W. Jia was on sabbatical leave away from Mayaguez Campus during 96-97 and back to UPR in 1997. He was carrying out the investigation of luminescent materials for long persistent phosphorescing and for low-voltage display. When he was on sabbatical he toke the opportunity to utilize the crystal growth facility available in UGA, screening a number of candidate materials to find some promising crystals. Dr. W. Jia received "Scholarly Productivity Award, The recognition of the most productive researchers in the EPSCoR project for 95-96, 97, 98-99, 00-01; and

"Scholarly Productivity Award, The recognition of the most productive researchers in UPR-Mayaguez.

3) Senior research scientist,
a. Yanyung Wang:
She started to work on this project in August, 1996 and partly supported or compensated by this grant. She is routinely preparing sol-gel materials and performing optical measurements every day.
b. Q. Yan was working for 2 years on nonlinear optical properties of niobate crystals and working on preparing inorganic glasses.

4) Other personnel:
Partly supported or shared by this grant,
1)Dr. Peter G. Zverev, Research associate, working on vibrational dynamic of crystal.
2)Dr. J.Zhang, Research associate, working on KNSBN materials.
3) Dr. Valentine Vikhnin, visiting scientist from Ioff Institute of Physics, Russia. He is specialized in exciton dynamics in solid state materials.
4) Dr. J. Yu, Postdoctor and visiting scientist, working in nanoparticle materials.
5) Dr. Sergey Avanesyan, research associate, working on ultrafast spectroscopy of solids.

5) Students:
Graduate Students:
1) Lymari Castro Diaz, MS Graduate student, Department of Physics, University of Puerto Rico, Mayaguez, PR 00681-9016. She was working on Cr or Eu-doped sol-gel optical materials. She received "Enrico Fermi" Best Student Award in UPR 1997. After 1.5 years working in this project she transferred to Cornel University for advanced degree study.
2) Carlos Rozo, MS student, graduated in May, 1997
3) Y. Fu, MS student, Thesis title "Nonlinear optical properties of SBN crystal", Graduated in May, 1998.
4) K. Ni, MS student, Thesis title "On the use of FFTS for the determination of the third-order nonlinearity for optical materials", Graduated in May, 2000.
5) Aziz Mahfoud Familia, MS Graduate student, Thesis title "Spectroscopic studies on Eu-doped silicon nanostructured optical materials", Graduated in May 2001
6) Miguel Santiago Rivera, MS student, working on "Preparation and Spectroscopic Study of Eu^{3+} doped and Eu^{3+}-Y^{3+} codoped Sol-Gel SiO_2 Glass". To be graduated in August 2001.
7) Iris Rivera Figueroa, MS student, working on "Laser Spectroscopy of Phosphor $CaTiO_3$:Pr^{3+}" graduated in August, 2001.
8) Karem Monge, MS student, working on "Laser Spectroscopy of Phosphor materials" to be graduated in August 2001.
9) Armando Yance Orcasita, MS Graduate student, He is currently working on Eu-doped high-melting point silicate ceramics for optical memory applications. He is scheduled to graduate in May 2002
10) Omar Vazquez Mata, MS student working on coherent passive optical limiting. This is the first year he started.

Undergraduate Students involved:
All the following students were involved and partly supported by the grant in this project. All of them were working in our Lab part-time.
Luciant Wolfsberger; Ivan E.Ramirez Hernandez; Crlos R.Reyes Rodriguez; Josue Maldonado; Eduardo Luiggi Lopez, German Garcia Cabrera, Carlos Reyes Rodriguez; Caroline E. Acosta, Kathia A Miranda, Lilybett M. Arcelay, David E. Quinones, Meredith Borrero Ramirez, Caroline E. Acosta, Kathia A Miranda, Lilybett M. Arcelay, David E. Quinones, Meredith Borrero Ramirez.

6. REPORT OF INVENTIONS

Two pending US patent applications were filed with joint ownership of the University of Puerto Rico and The University of Georgia:

1) " Long Persistence blue phosphors", US patent 6,117,362

2) "Phosphors with long persistent green phosphorescence", US patent application number: 09/187,943, pending

7. BIBLIOGRAPHY

1. H.Liu, F. Fernandez, W.Jia, L.A.Boatner, SPIE Proc.,Vol. 3425 (1998)182. .
2. F.E. Fernández, H. Liu, C. Jin, and W. Jia, Integrated Ferroelectrics (1999), in press.
3. R.M.Macfarlane and R.M. Shelby, in *Spectroscopy of Solids Containing Rare-Earth ions*, ed., by A.A. Kaplyanskii and R.M. Macfarlane (North-Holland, Amsterdam, 1987), p.51.
4. K. Fujita, K. Tanaka, K. Hirao and N. Soga, Opt.Lett., 23 (1998) 543.
5. H.Liu, R.C.Powell and L.A.Boatner, J.Appl.Phys., **70** (1991) 20.
6. H. Liu, W. Jia and L.A. Boatner, SPIE Proc. Vol. 3491, (1998)745.
7. V. Petricevic, S.K. Gayen and R.R. Alfano, Appl. Phys. Lett., 53 (1988) 2590.
8. H. Ellers, W.M. Dennis, W.M. Yen, S. Kock, K. Peterman, G. Huber and W. Jia, IEEE J. Quant. Electron., 29 (1993) 2508.
9. L.D. DeLoach, R.H. Page, G.D. Wilke, S.A. Payne, and W.F. Krupe, OSA Procedings on Advanced Solid State Lasers, 24 (1995) 127.
10. J.P. Meyn, T. Danger, K. Peterman and G. Huber, J. Lumin., 55 (1993) 55.
11. N.S. Garif'yanov, Soviet Physics-Solid State, 4 (1963) 1795.
12. K. Tanaka and K. Kamiya, J. Mat. Scien. Lett., 10 (1991) 1095.
13. M. Herren, H. Nishiuchi, and Morita, J. Chem. Phys., 101 (1994) 4461.
14. M. Herren, K. Yamanaka and M. Morita, Technical Reports of Seikei University, 32, No.2 (1995) 61.
15. Huabiao Yuan, Weiyi Jia, D. Cohen, W.M. Yen and B.G. Aiken, Mat. Res. Soc. Symp. Proc., 455 (1997) 483.
16. C.J. Brinker and G.W. Scherer, the Physics and Chemistry of Sol-Gel Processing, the third edition, Academic Press, San Diego, 1990.
17. P.F. Moulton, J. Opt. Soc. Am. B, 3 (1) (1986) 125.
18. Macfarlane, R.M., and Shelby, R.M., *Spectroscopy of Solids Containing Rare-Earth ions"*, ed., by Kaplyanskii, A.A., and Macfarlane, R.M., Amsterdam, North-Holland, 1987, p.51.
19. Yano. R., Mitsunaga, M., and Uesugi, N., J.Opt.Soc.Am.B, **9**, 992 (1992).
20. Kogelink, H., Bull. Syst. Tech. J. **48,** 2909 (1969).
21. Liu, H., Reeves, R.J., Powell, R.C., and Boatner, L.A., Phys.Rev., **49**, 6323 (1994), **.44,** 2461 (1991).
22. Seglins, J., and Kapphan, S., Phys.Stat.Sol.(b), **188**, K43 (1995).
23. Neurgaonkar, R.R., Cory, W.K., Oliver, J.R., Ewbank, M.D., Hall, W.F., Opt.Eng., **26**, 392 (1987).
24. P. Günter, E. Voit, M. Z. Zha, and J. Albers, "Self-pulsation and optical chaos in self-pumped photorefractive $BatiO_3$", Opt. Commun. 55, 210-215 (1985).
25. B. A. Wechsler, M. B. Klein, C. C. Nelson, and R. N. Schwartz, "Spectroscopic and photorefractive properties of infrared-sensitive rhodium-doped barium titanate", Opt. Lett. 536-538 (1994).
26. S. Bian, J. Zhang, X. Su, K. Xu, Q. Jiang, H. Chen, and D. Sun, "Self-pumped phase conjugation of 18°-cut Ce-doped KNSBN crystal at 632.8nm" , Opt. Lett. 18, 769-771 (1993).
27. Q. Jiang, X. Lu, Y. Song, D. Sun, H. Chen, "Copper-ion point defects in the photorefractive material $(K_xNa_{1-x})_{0.4}(Sr_yBa_{1-y})_{0.8}Nb_2O_6$", Phys. Rev. B 50, 4185-4188 (1994).

28. J. Feinberg, "Self-pumped, continuous-wave phase conjugator using reflection", Opt. Lett. 7, 486-488 (1982).
29. A. Krumins, A. Anspokes, S. G. Odoulov, J. Seglines, P. Vaivods, "Thermal holograms in doped ferroelectric SBN crystals", Ferroelectrics 80, 277-280 (1988).
30. G. A. Brost, R. A. Motes, and J. R. Rotge, "Intensity-dependent absorption and photorefractive effects in barium titanate", J. Opt. Soc. Am. B 5, 1879-1885 (1988).
31. K. Buse, K. H. Ringhofer, "Pyroelectric drive for light-induced charge transport in the photorefractive process", Appl. Phys. A 57, 161-165 (1993).
32. K. Buse, "Thermal gratings and pyroelectrically produced charge redistribution in $BaTiO_3$ and $KNbO_3$", J. Opt. Soc. Am. B 10, 1266-1275 (1993).
33. F. Jermann, K. Buse, " Light-induced thermal gratings in $LiNbO_3$:Fe", Appl. Phys. B 59, 437-443 (1994).
34. R. R. Neurgaonkar, W. K. Cory, J. R. Oliver, M. D. Ewbank, and W. F. Hall, "Development and modification of photorefractive properties in the tungsten bronze family crystals", Opt. Eng. 26, 392-405 (1987).
35. T. Tschudi, A. Herden, J. Goltz, H. Klumb, F. Laseri, and J. Albers, "Image amplification by two- and four-wave mixing in $BaTiO_3$ photorefractive crystals", IEEE J. Quantum Electron. QE-22, 1493-1502 (1986).
36. Z.C. Feng and R. Tsu, Porous Silicon (World Scientific, Singapore, 1994).
37. Hideki Koyama, Ysuyoshi Ozaki, and Nobuyoshi Koshida, Phys. Rev. 52, 11561 (1995).
38. H. Koyama and N. Koshida, Phys. Rev. B 52, 2649 (1995).
39. J.P. Bourdin, P.X. Nguyen, G. Rivoire and J.M. Nunzi, Nonlinear Opt., 7, 1 (1994).
40, G. Fasol, H. P. Hughes, Phys. Rev. B 33 (1996) 2953.
41, K. K. Rebane and P. M. Saari, Soviet Physics-Uspekhi 19 (1976) 959.
42, Weiyi Jia and W.M.Yen, Phys. Rev.,25 (1982) 6006.
43, K. Z. Troost, M. J. van Dort, J. I. Dijkhuis, and H. W. de Wijn, Phis.Rev. B 43 (1991) 98. Green Phosphorescence" (87-97P) and "Long Persistence Blue Phosphors" (88-97P)
44. Huimin Liu, L. F. Fonseca, S. Z. Weisz , W. Jia and O. Resto, *J. Lumin.*, 83-84, 37 (1999).
45. Huimin Liu, Aziz Mahfoud, G.A. Nery, Luis F. Fonseca, O. Resto and Zvi S. Weisz, "*Photoluminescence of Eu^{3+} in Si/SiO_2 nanostructure films*" *Proc. MRS*, Vol.609, Spring meeting, San Francisco, (2000).
46. J. Sik, M. Schubert, G.Leibiger, V. Gottschalch, *J. Appl. Phys.* **89**, 294 (2001).
47. Y. G. Semenov, S. M. Ryabchenko, *Low Temp.Phys.*, **26**, 886 (2000).
48. H.Liu, R.J.Reeves, R.C.Powell, L.A.Boatner, *Phys.Rev.B,* **49**, 6323 (1994).
49. V. Vikhnin, H.Liu, W.Jia, *Phys.Letters A*, **245**, 307 (1998); *Ferroelectrics*, **237**, 81 (2000).
50. V.S. Vikhnin, H. Liu, W. Jia. Ferroelectrics, accepted for publication (1999); Phys. Letters A, in press (1999); Phys. Letters A, 245, 307 (1998).
51. V.S. Vikhnin. Proc. Est. Acad. Sci., Phys., Math., 44(2/3), 164 (1995); Ferroelectrics, 199, 25 (1997); Z. Phys. Chem, 201, 201 (1997); Ferroelectric Letters, 25, no. 1/2 (1999).
52. H. Liu, R.C. Powell, L.A. Boatner. J.Appl.Phys.,70(1),20(1991);Phys.Rev.B,44,2461 (1991).
53. Liu, H., Reeves, R.J., Powell, R.C. and Boatner, L.A. *Phys. Rev.* **B 49**, (1994) 6323.
54. Limonov, M.F., Kapphan, S., Vikhnin, V.S., Laisheva, L.V., Hesse, H., Krivospitskii , A.N. and Smirnov, M.B.. *Z. Phys. Chem.* **201**,(1997) 215.
55. Voigt, P. and Kapphan, S.. *J. Phys. Chem. Solids*, **55**, (1994) 853.
56. V.S.Vikhnin. Proc. Est. Acad. Sci., Phys., Math., 44(2/3), 164 (1995)
57. V.S.Vikhnin. Ferroelectrics, 199, 25 (1997); Z. Phys. Chem., 201, 201 (1997)
58. V.S.Vikhnin. Ferroelectric Letters, 25, no. ½ (1999)
59. V.S.Vikhnin, S.Kapphan, J.Seglins. Rad. Eff. and Def. in Sol., to be published (1999)
60. M.F.Limonov, S.Kapphan, V.S.Vikhnin et al, Z. Phys. Chem., 201, 215 (1997)
61. C. auf der Horst, J.Leiher, S.Kapphan, V.Vikhnin, S.Prosandeyev. To be published (1999)
62. V.Vikhnin, D.Usvayt, M.Limonov, M.Smirnov. Sol. St. Comm., to be published (1999)

8. REPORT OF INVENTIONS

None.